UNIVERSITY OF LEEDS

This is a repository copy of *The influence of metabolic and circulatory heterogeneity on the expression of pulmonary oxygen uptake kinetics in humans*.

White Rose Research Online URL for this paper:
http://eprints.whiterose.ac.uk/91938/

Version: Accepted Version

Article:
Keir, DA, Robertson, TC, Benson, AP et al. (2 more authors) (2016) The influence of metabolic and circulatory heterogeneity on the expression of pulmonary oxygen uptake kinetics in humans. Experimental Physiology, 101 (1). pp. 176-192. ISSN 0958-0670

https://doi.org/10.1113/EP085338

Reuse
Unless indicated otherwise, fulltext items are protected by copyright with all rights reserved. The copyright exception in section 29 of the Copyright, Designs and Patents Act 1988 allows the making of a single copy solely for the purpose of non-commercial research or private study within the limits of fair dealing. The publisher or other rights-holder may allow further reproduction and re-use of this version - refer to the White Rose Research Online record for this item. Where records identify the publisher as the copyright holder, users can verify any specific terms of use on the publisher's website.

Takedown
If you consider content in White Rose Research Online to be in breach of UK law, please notify us by emailing eprints@whiterose.ac.uk including the URL of the record and the reason for the withdrawal request.

White Rose university consortium
Universities of Leeds, Sheffield & York

eprints@whiterose.ac.uk
https://eprints.whiterose.ac.uk/

The influence of metabolic and circulatory heterogeneity on the expression of pulmonary $\dot{V}O_2$ kinetics in humans

Daniel A. Keir[1,2], Taylor C. Robertson[1,2], Alan P. Benson[4], Harry B. Rossiter[5], & John M. Kowalchuk[1,2,3]

[1]Canadian Centre for Activity and Aging, [2]School of Kinesiology, [3]Department of Physiology and Pharmacology, The University of Western Ontario, London, ON, Canada, [4]School of Biomedical Sciences, University of Leeds, Leeds, United Kingdom, and [5]Rehabilitation Clinical Trials Center, Division of Respiratory & Critical Care Physiology & Medicine, Los Angeles Biomedical Research Institute at Harbor-UCLA Medical Center, Torrance, CA, USA.

Running Title: $\dot{V}O_{2p}$ kinetics are slowed dependent on the pre-transition work rate

Key words: O_2 uptake kinetics, near-infrared spectroscopy, metabolic rate, muscle

Corresponding author: Dr. J. M. Kowalchuk
School of Kinesiology
The University of Western Ontario
London, Ontario, Canada
N6A 3K7
e-mail: jkowalch@uwo.ca
phone: (519) 661-1605

New findings

What is the central question of this study?

That pulmonary $\dot{V}O_2$ kinetics on transition to moderate exercise is invariant and exponential is consistent with a first-order reaction controlling $\dot{V}O_2$. However, slowed $\dot{V}O_2$ kinetics when initiating exercise from raised baseline intensities challenges this notion.

What is the main finding and its importance?

Here we demonstrate how a first-order system can respond with non-first-order response dynamics. Data suggest that progressive recruitment of muscle fibre populations having progressively lower mitochondrial density and slower microvascular blood flow kinetics can unify the seemingly contradictory evidence for the control of pulmonary $\dot{V}O_2$ on transition to exercise.

Abstract

We examined the relationship amongst baseline work rate (WR), phase II pulmonary $\dot{V}O_2$ time constant ($\tau\dot{V}O_{2p}$) and functional gain (G_P: $\Delta\dot{V}O_{2p}/\Delta WR$) during moderate-intensity exercise. Transitions were initiated from a constant or variable baseline WR. A validated circulatory model was used to examine the role of heterogeneity in muscle metabolism ($\dot{V}O_{2m}$) and blood flow ($\dot{Q}_m$) in determining $\dot{V}O_{2p}$ kinetics. We hypothesized that $\tau\dot{V}O_{2p}$ and G_P would be invariant in the constant baseline condition, but would increase linearly with increased baseline WR. Fourteen men completed 3-5 repetitions of Δ40W step-transitions initiated from 20, 40, 60, 80, 100, and 120 W on a cycle ergometer. The Δ40W step-transitions from 60, 80, 100, and 120 W were preceded by 6 minutes of 20 W cycling from which the progressive ΔWR transitions (constant baseline condition) were examined. $\dot{V}O_{2p}$ was measured breath-by-breath using mass spectrometry and volume turbine. For a given ΔWR, both $\tau\dot{V}O_{2p}$ (22 to 35s) and G_P (8.7 to 10.5 $mL \cdot min^{-1} \cdot W^{-1}$) increased ($p<0.05$) linearly as a function of baseline WR (20 to 120 W). $\tau\dot{V}O_{2p}$ was invariant ($p<0.05$) in transitions initiated from 20 W, but G_P increased with ΔWR ($p<0.05$). Modeling the summed influence of multiple muscle compartments revealed that $\tau\dot{V}O_{2p}$ could appear fast (24s), and similar to *in vivo* measurements (22±6s), despite being derived from $\tau\dot{V}O_{2m}$ values ranging 15-40s and $\tau\dot{Q}_m$ ranging 20-45s suggesting that within the moderate-intensity domain phase II $\dot{V}O_{2p}$ kinetics are slowed dependent on the pre-transition WR, and are strongly influenced by muscle metabolic and circulatory heterogeneity.

Introduction

After a step-change in moderate-intensity exercise work rate (WR) (i.e., below the lactate threshold), pulmonary O_2 uptake ($\dot{V}O_{2p}$) increases in an exponential-like manner towards a new steady-state O_2 requirement following a brief cardiodynamic period (phase I). The exponential increase in $\dot{V}O_{2p}$ (phase II) is closely associated with the dynamic adjustment of skeletal muscle $\dot{V}O_2$ ($\dot{V}O_{2m}$) (Barstow *et al.* 1990; Grassi *et al.* 1996; Krustrup *et al.* 2009) and is characterized by both its rate (quantified by the time constant for $\dot{V}O_{2p}$ [$\tau\dot{V}O_{2p}$]) and amplitude (quantified by the functional $\dot{V}O_{2p}$ gain [G_P: $\Delta\dot{V}O_{2p}/\Delta WR$]) (Whipp *et al.* 1982).

During exercise initiated from a common, low, baseline WR, both phase II $\tau\dot{V}O_{2p}$ and G_P are invariant, and independent of the subsequent moderate-intensity WR performed (Özyener *et al.* 2001; Spencer *et al.* 2013). This kinetic behavior implies that phase II $\dot{V}O_{2p}$ kinetics are consequent to a first order rate reaction; specifically, linked, to mitochondrial ADP feedback (Rossiter, 2011; Wüst *et al.* 2011). However, when exercise is initiated from a raised baseline WR and metabolic rate, $\dot{V}O_{2p}$ kinetics are slowed: both $\tau\dot{V}O_{2p}$ and G_P are increased (Brittain *et al.* 2001; MacPhee *et al.* 2005; Spencer *et al.* 2011; Bowen *et al.* 2011; Williams *et al.* 2013; Keir *et al.* 2014). This behavior was suggested to be evidence that $\dot{V}O_{2p}$ kinetics do not conform to a first order rate reaction (Robergs, 2014). However, others interpreted this kinetic slowing to be reflective of the physiological properties of the activated musculature (Brittain *et al.* 2001), where individual fibers operate through a first-order ADP-feedback reaction, but where mitochondrial volume-density differs among the activated muscle fibers (Rossiter, 2011). In other words, preferential activation of highly oxidative muscle fibers at low baseline WR will have inherently faster $\dot{V}O_{2p}$ kinetics than less-oxidative fibers activated at higher work rates; yet within each fiber $\dot{V}O_{2p}$ kinetics are first order (Brittain *et al.* 2001).

Recently, Keir *et al.* (2014) reported that moderate-intensity $\dot{V}O_{2p}$ kinetics were strongly related to baseline metabolic rate, but not to the baseline WR or the magnitude of the increase in WR during the exercise bout (ΔWR). This suggested that the intramuscular metabolic status (e.g. [ADP]/[ATP], and/or free energy of ATP), rather than kinetic characteristics of the recruited motor units, influence $\dot{V}O_{2p}$ kinetics; a conclusion supported by Bowen *et al.* (2011) using a model of incomplete muscle recovery, and by Wüst *et al.* (2014) with exercise transitions in electrically-stimulated dog hind limb muscle. However, DiMenna *et al.* (2010), using high-intensity exercise, found that baseline metabolic rate did not influence subsequent $\dot{V}O_{2p}$ kinetics, supporting the recruitment hypothesis.

To shed light on this controversy we aimed to determine the relationship between baseline metabolic rate and $\dot{V}O_{2p}$ kinetics during exercise initiated from several different rates of baseline metabolism, each using an identical work rate increment (ΔWR) within the moderate-intensity domain; previous investigations having used only two different baseline work rates. This would allow us to determine whether $\dot{V}O_{2p}$ kinetics are slowed in relation to baseline $\dot{V}O_{2p}$. Additionally, to account for potential confounding effects of regional O_2 delivery on muscle $\dot{V}O_{2p}$ (Hughson & Morrissey, 1982; MacPhee *et al.* 2005; Koga *et al.* 2007; Wüst *et al.* 2014), we simultaneously measured regional muscle deoxygenation (hemoglobin (Hb) + myoglobin (Mb); hereafter referred to as "[HHb]") by near-infrared spectroscopy, which reflects the relationship between microvascular O_2 delivery to O_2 utilization (Murias *et al.* 2014). In addition, it is well understood that $\dot{V}O_{2m}$ kinetics can be modulated by circulatory dynamics on transition to their pulmonary expression as phase II $\dot{V}O_{2p}$ (Hoffmann *et al.* 2013; Benson *et al.* 2013). To account for this we used a validated circulatory model (Benson *et al.* 2013) to determine whether

104 circulatory distortions could explain a progressive slowing of $\dot{V}O_{2p}$ kinetics with progressively
105 greater baseline work rate.

106 Thus, the purpose of this study was to determine in the same participants: 1) $\dot{V}O_{2p}$ and
107 [HHb] kinetics over a range of moderate-intensity WR increments initiated from a constant
108 baseline metabolic rate, i.e., the same baseline metabolism with variable ΔWR (constant baseline
109 condition); 2) the relationship between baseline metabolic rate and $\dot{V}O_{2p}$ and [HHb] kinetics for
110 a constant WR increment within the moderate-intensity domain, i.e., variable baseline
111 metabolism with the same ΔWR (variable baseline condition); and 3) the extent to which
112 circulatory dynamics may contribute to the slowed $\dot{V}O_{2p}$ kinetics from progressively increasing
113 baseline metabolic rate. We hypothesized that, unlike in the constant baseline condition, in the
114 variable baseline condition $\tau\dot{V}O_{2p}$ and G_P would increase linearly with baseline $\dot{V}O_{2p}$
115 independent of [HHb] dynamics, and that these differences could not be explained by circulatory
116 modulation of muscle $\dot{V}O_2$ kinetics. Accepting this hypothesis would suggest an association
117 between instantaneous muscle metabolism and $\tau\dot{V}O_{2p}$ and G_P in moderate intensity exercise,
118 which is inconsistent with simple first order kinetic control theory.

119

120 **Methods**

121 *Ethical approval.* The study was conducted according to the Declaration of Helsinki and all
122 procedures were approved by The University of Western Ontario Ethics Committee for Research
123 on Human Subjects. All participants volunteered and gave informed written consent to
124 participate in the study.

125

126 *Participants.* Fourteen healthy young adult men (mean ± SD values: age, 24 ± 3 yrs; body mass,
127 83 ± 5 kg; height, 180 ± 8 cm; $\dot{V}O_{2peak}$, 48.1 ± 5.9 $mL \cdot kg^{-1} \cdot min^{-1}$) volunteered for the study. All
128 participants were non-smokers who were free of any known musculoskeletal, respiratory,
129 cardiovascular, and metabolic conditions, and who were not taking any medications that might
130 influence cardiorespiratory or metabolic responses to exercise. Participants were selected on the
131 basis that their WR at the estimate lactate threshold ($\hat{\theta}_L$) was at least 130 W, allowing all step-
132 transitions used in the protocol to begin within the moderate-intensity domain.
133
134 *Ramp Incremental Exercise.* Each participant reported to the laboratory to perform a symptom-
135 limited ramp incremental (RI) exercise test (20 W baseline for 4 min followed by a 25 $W \cdot min^{-1}$
136 ramp) on a magnetically-braked cycle ergometer (model: Velotron, RacerMate Inc., Seattle, WA,
137 USA) for determination of peak $\dot{V}O_{2p}$ ($\dot{V}O_{2peak}$) and peak WR (WR_{peak}). Participants were asked
138 to maintain a cadence of ~60 rpm during the test. $\dot{V}O_{2peak}$ was defined as the greatest 20 s $\dot{V}O_{2p}$
139 computed from a rolling average and WR_{peak} was defined as the WR achieved at termination of
140 the RI test. Additionally, the $\hat{\theta}_L$ was determined by visual inspection using standard ventilatory
141 and gas exchange indices as previously described (Beaver *et al.* 1986).
142
143 *Constant Work Rate Exercise Protocols.* Participants performed 3-5 repetitions of 40W step-
144 increments (i.e., Δ40) from a baseline WR of 20, 40, 60, 80, 100, and 120 W (i.e., variable
145 baseline condition). Step-transitions were 6 min of baseline WR followed by an instantaneous
146 step-increase in WR to 40 W above the baseline for 6 min. With the exception of the step-
147 transitions from 20 W and 40 W, all other transitions were preceded by 6 min of baseline cycling
148 at 20 W, which provided an opportunity to examine step-transitions from a common 20 W

baseline and different WR increments (i.e., Δ40, Δ60, Δ80, Δ100; constant baseline condition). Therefore, one-third of the exercise protocols were 12 min in duration (those initiated from 20 and 40 W) and the other two-thirds were 18 min (see Figure 1). A maximum of two exercise protocols were completed per visit with a minimum of 20 min seated rest between exercise bouts. For each participant, the sequence of exercise protocols was randomized in a counterbalanced order and it was assumed that exercise duration did not affect physiological outcome measures.

Data Collection. During each trial participants wore a noseclip and breathed through a mouthpiece for breath-by-breath gas-exchange measurements. Inspired and expired volumes and flow rates were measured using a low dead space (90 mL) bidirectional turbine (Alpha Technologies, VMM 110) and pneumotach (Hans Rudolph, Model 4813) positioned in series from the mouthpiece (total apparatus dead space was 150 mL); respired air was continuously sampled at the mouth and analysed by mass spectrometry (Innovision, AMIS 2000, Lindvedvej, Denmark) for fractional concentrations of O_2 and CO_2. The volume turbine was calibrated before each test using a syringe of known volume (3 L) over a range of flow rates and the pneumotach was adjusted for zero flow. Gas concentrations were calibrated with precision-analyzed gas mixtures. The time delay between an instantaneous, square-wave change in fractional gas concentration at the sampling inlet and its detection by the mass spectrometer was measured electronically by computer. Respiratory volumes, flow, and gas concentrations were recorded in real-time used to build a profile of each breath. Alveolar gas exchange was calculated on a breath-by-breath basis using the algorithms of Swanson (1980).

Local muscle deoxygenation ([HHb]) of the quadriceps *vastus lateralis* muscle was measured using a frequency domain multi-distance near-infrared spectroscopy (NIRS) system

(Oxiplex TS, Model 92505, ISS, Champaign, USA) as described elsewhere (Spencer *et al.* 2012). Briefly, the system was comprised of a single channel consisting of eight laser diodes operating at two wavelengths (λ = 690 and 828 nm, four at each wavelength) that were pulsed in a rapid succession down a photomultiplier tube. A rigid plastic NIRS probe (connected to laser diodes and photomultiplier tube by optical fibers) consisted of two parallel rows of light emitter fibers and one detector fiber bundle; the source-detector separations for this probe were 2.0, 2.5, 3.0, and 3.5 cm for both wavelengths. The probe was placed on the belly of the muscle, at the distal end of the *vastus lateralis* muscle. NIRS measurements were collected continuously for the entire duration of each trial. The NIRS was calibrated at the beginning of each testing session following an instrument warm-up period of at least 20 min. Throughout each testing session, continuous measurements of the absolute scattering (μ_s) and absorption (μ_a) coefficients for each wavelength were determined by measuring the intensity of modulated light entering and traversing the tissue (determined from the average component of the modulated light waves [DC], amplitude of the modulation [AC], and the phase shift [Φ] between those two signals) at the four source - detector distances (R). The coefficients of AC and Φ were plotted as a function of distance R at both wavelengths to determine μ_s and μ_a, which were used to resolve the absolute concentrations of HHb (in μM) using the Beer-Lambert equation. Data were stored online at an output frequency of 25 Hz, but were reduced to 1 s bins for all subsequent analyses.

Data Analysis. Breath-by-breath $\dot{V}O_{2p}$ data were edited on an individual basis by removing aberrant data that lay 3 SD from the local mean (Lamarra *et al.* 1987). Within each participant, like-repetitions were linearly interpolated on a second-by-second basis, ensemble-averaged and

194 time-aligned such that time "zero" represented the onset of the transition. The on-transient of
195 each profile was modeled with the following mono-exponential function:
196
197 $$y(t) = y_{BSL} + A \cdot (1 - e^{-(t\text{-}TD)/\tau}) \quad (1)$$
198
199 where, $y(t)$ is the value of the dependent variable at any time during the transition, y_{BSL} is the
200 pre-transition baseline value (determined from the ~60 s before a transition), A is the steady-state
201 increase in y above the baseline value, TD is the time delay, and τ is the time constant of the
202 response (or the time for y to increase to 63% of the new steady-state after TD). The functional
203 gain (G_P: $\Delta\dot{V}O_{2p}/\Delta WR$) of the response was determined by dividing A (in $mL \cdot min^{-1}$) by the
204 change in WR (in W). Data were fit using the Levenberg-Marquardt algorithm to find the
205 minimum sum of squared residuals between the mono-exponential function and the experimental
206 data (using Origin 8.5; OriginLab, Northampton, MA). The end of the fitting window was set to
207 ~ 5 times the estimated time constant in order to restrict the modeling to data lying within the
208 transient phase. For those individuals who transitioned into the heavy-intensity domain, the end
209 of the phase II fitting window was determined by examining the change in τ, CI_{95}, χ^2, and plotted
210 residuals in response to progressive increases in the end of the fitting window. The point
211 immediately preceding a systematic increase in τ, CI_{95}, and χ^2 was considered as the end of phase
212 II. The mean response time (MRT-$\dot{V}O_{2p}$) of $\dot{V}O_{2p}$ was characterized from a fit of the $\dot{V}O_{2p}$
213 response from t=0 to the end of the exercise
214 The TD for the [HHb] ([HHb]-TD) response was determined using second-by-second
215 data and corresponded to the time, after the onset of exercise, at which the [HHb] signal
216 increased above 1 SD of the pre-transition baseline value. Determination of the [HHb]-TD was

made on each individual's ensemble-averaged response and the data were modeled using equation 1. Different fitting strategies ranging from 90-180 s into a transition resulted in minimal differences in estimates of τ[HHb]. The MRT for [HHb] (MRT-[HHb]) described the overall time for [HHb] to increase from the start of exercise to 63% of the "steady-state" value and was calculated as the sum of τ[HHb] and [HHb]-TD.

In silico simulations. The validated multi-compartmental model (MCM) of Benson *et al.* (2013) was used to investigate the dissociation between muscle and pulmonary $\dot{V}O_2$ kinetics. Briefly, mathematical expressions for O_2 delivery ($\dot{Q}$), muscle O_2 uptake, and a lumped compartment representing the rest of the body were joined in parallel by a single arterial compartment and multiple compartments on the venous side (representing blood draining the muscle, the rest of the body, and a mixed compartment approximating the blood volume proximal to the common femoral veins). The fractions of total metabolic rate (from muscle: 0.57; from body 0.43) and cardiac output ($\dot{Q}$; to muscle: 0.57; to body 0.43) for unloaded pedaling and venous blood volume associated with muscle (0.7 L), body (0.1 L), and mixed compartments (2.3 L) were fixed while the WR and kinetic variables for muscle and body $\dot{Q}$ ($\dot{Q}_m$ and $\dot{Q}_b$) and $\dot{V}O_2$ ($\dot{V}O_{2m}$ and $\dot{V}O_{2b}$) were manipulated experimentally to mimic the pre-transition conditions of the *in vivo* experiments and predict phase I and phase II $\dot{V}O_{2p}$ kinetics. The output of the model was instantaneous $\dot{V}O_{2p}(t)$:

$$\dot{V}O_{2p}(t) = \dot{Q}(t) \cdot (C_aO_2 - C_{\bar{v}}O_2)(t) \quad (2)$$

where C_aO_2 is arterial content (fixed to 20 mL O_2 per 100 mL of blood), $C_{\bar{v}}O_2$ is mixed venous O_2 content. During the simulated exercise step-transitions, $\dot{Q}_m$ and $\dot{V}O_{2m}$ increased exponentially according to equation 1 (with TD = 0), toward their WR-dependent steady-state values with a steady-state relationship of 6 $L \cdot min^{-1}$ per 1 $L \cdot min^{-1}$ of $\dot{V}O_2$. The intercept of the $\dot{Q}$-to-$\dot{V}O_2$ relationship was set to 3.6 $L \cdot min^{-1}$ (Benson *et al.* 2013). Values of $\dot{V}O_2$ were dependent on WR inputs and functional gains (i.e., $\Delta\dot{V}O_2/\Delta W$) of 9.5, 11.0, and -1.5 $mL \cdot min^{-1} \cdot W^{-1}$ for $\dot{V}O_{2p}$, $\dot{V}O_{2m}$, and $\dot{V}O_{2b}$, respectively as previously described (Benson *et al.* 2013). Values for $\dot{Q}$ in the various compartments were based on the aforementioned $\dot{Q}$-to-$\dot{V}O_2$ relationship.

Exercise was simulated for moderate-intensity transitions by specifying a step-change in WR. Initially, the steady-state $\dot{V}O_{2p}$ baseline for 20 W was set to 0.75 $L \cdot min^{-1}$ and $\tau\dot{V}O_{2m}$ and $\tau\dot{Q}_m$ were modulated in order to generate a $\tau\dot{V}O_{2p}$ value that corresponded to the group mean $\tau\dot{V}O_{2p}$ from the 20 W to 60 W step. Thereafter, simulations were done for Δ40W step-changes from 40, 60, 80, 100, and 120 W and for Δ60W, Δ80W, and Δ100W step-changes from 20 W with fixed parameter inputs for $\tau\dot{V}O_{2m}$ and $\tau\dot{Q}_m$ in order to determine the degree by which circulatory dynamics modulate the dynamics of $\dot{V}O_{2p}$ at a constant $\tau\dot{V}O_{2m}$ and varying moderate-intensity baseline WR and WR increments. In addition, simulations were produced to examine the influence of slowing $\dot{Q}_m$ dynamics on the $\dot{V}O_{2p}$ profile; for each of the Δ40W step-changes, $\tau\dot{V}O_{2m}$ was fixed to each of 20, 30, and 40 s, and a series of simulations of $\dot{V}O_{2p}$ was produced where $\tau\dot{Q}_m$ was varied (MacPhee *et al.* 2005). In all experimental conditions, the phase II region of the $\dot{V}O_{2p}$ output from the simulations was fitted to equation 1, with the end of phase I being identified precisely from the profile of simulated $C_{\bar{v}}O_2$.

To investigate how the homogenized $\dot{V}O_{2p}$ response to a step-change in WR from 20 to 120 W may be influenced by multiple muscle compartments with heterogeneous metabolic and

circulatory dynamics, the group mean dynamic responses of $\dot{V}O_{2p}$ and [HHb] from each of the equal WR increment steps (variable baseline condition) were used to infer the $\dot{V}O_{2m}$ and $\dot{Q}_m$ kinetics of six theoretical muscle compartments ($\tau\dot{V}O_{2m}$ = 15, 20, 25, 30, 35, 40 s and $\tau\dot{Q}_m$ = 20, 25, 30, 35, 40, 45 s for compartments 1 – 6, respectively) assuming that both $\tau\dot{V}O_{2m}$ and $\tau\dot{Q}_m$ linearly increase as a function of WR. Assuming simultaneous activation and equal contributions of each of the six compartments, the homogenized $\dot{V}O_{2p}$ response to a step-change in WR from 20 to 120 W was simulated for each compartment and combined into a single homogenized response. The averaged $\dot{V}O_{2p}$ output was modeled as previously mentioned and kinetics were compared to the actual group mean $\dot{V}O_{2p}$ response to the step-change in WR from 20 to 120 W.

Statistical Analysis. Data are presented as means ± SD. A one-way analysis of variance (ANOVA) for repeated measures was used to compare kinetic parameters and variables between conditions. Where significant main effects were found, a Tukey's *post hoc* analysis was performed for multiple comparisons testing. All statistical analyses were performed using SigmaPlot Version 11.0, (Systat Software Inc., San Jose, CA). Statistical significance was accepted at an alpha level of 5%.

Results

The group mean $\hat{\theta}_L$ was 2.22 ± 0.32 L·min^{-1} (range: 1.85 – 3.00 L·min^{-1}), which corresponded to a mean WR of 161 ± 34 W (range: 130 – 240 W). Therefore, the WR associated with $\hat{\theta}_L$ for all participants was greater than the maximum baseline WR from which step-transitions were initiated in the experimental protocol (i.e., 120 W). The 40 W transitions from baselines of 20, 40, 60, 80, 100, and 120 W corresponded to 35 ± 6, 43 ± 7, 51 ± 8, 60 ± 9, 68 ±

285 10, 78 ± 12 % of $\dot{V}O_{2p}$ at $\hat{\theta}_L$, and the steady-state $\dot{V}O_{2p}$ achieved corresponded to 50 ± 8, 60 ± 9,
286 68 ± 10, 78 ± 11, 87 ± 12, 97 ± 14 % of $\hat{\theta}_L$. Based on the steady-state $\dot{V}O_{2p}$ achieved, four (of
287 14) participants transitioned into the heavy-intensity domain at 160 W and one at 140 W.
288 However, removal of these data *post hoc* did not alter the overall study outcomes described
289 below.

290 Table 1 shows the phase II $\dot{V}O_{2p}$ parameters for each of the variable baseline conditions.
291 The ensemble-averaged group profiles of $\dot{V}O_{2p}$ for the variable baseline condition are displayed
292 in Figure 2. In each panel, a mono-exponential fit derived from the group mean parameter
293 estimates (from equation 1) is superimposed over the data. As designed, $\dot{V}O_{2pBSL}$ increased
294 ($p<0.05$) progressively from the 20 W to 120 W baseline transitions (Table 1). Despite constant
295 ΔWR, the parameter estimates for A, G_P and $\tau\dot{V}O_{2p}$ increased progressively with increasing
296 baseline WR ($p<0.05$; see Table 1 and Figure 3 for pairwise differences).

297 The group mean parameter estimates from the phase II $\dot{V}O_{2p}$ fits for the constant baseline
298 condition exercise transitions are displayed in Table 2. Figure 4 shows the mean $\dot{V}O_{2p}$ responses
299 for Δ40, Δ60, Δ80, Δ100 W transitions from a 20 W baseline. As designed, $\dot{V}O_{2pBSL}$ did not
300 change ($p>0.05$) amongst these step-transitions and A increased ($p<0.05$) with increasing WR
301 increment. The G_P increased ($p<0.05$, main effect) during transitions to increasing moderate-
302 intensity WRs, but there was no difference in $\tau\dot{V}O_{2p}$ among the different ΔWR conditions
303 ($p>0.05$). The relationships between A, $\tau\dot{V}O_{2p}$ or G_P, and the WR increment are shown in Figure
304 5.

305 The kinetic parameters of [HHb] under the variable and constant baseline conditions are
306 shown in Tables 3 and 4 with group mean responses displayed in Figures 6 and 7. Similar to
307 $\dot{V}O_{2p}$, τ[HHb] increased with increasing $\dot{V}O_{2pBSL}$ ($p<0.05$, main effect). Baseline [HHb]

increased ($p<0.05$, main effect) and [HHb]-TD decreased ($p<0.05$, main effect) with increasing baseline WR (see Table 3 for multiple comparisons). The Δ[HHb] and MRT-[HHb] were not different ($p>0.05$) when the WR increment was constant (variable baseline condition; Table 3) but, as expected, Δ[HHb] increased ($p<0.05$) with increasing ΔWR (constant baseline condition; Table 4). There was no influence of WR increment ($p>0.05$) on $[HHb]_{BSL}$, [HHb]-TD, MRT-[HHb], or τ[HHb] in the constant baseline condition (Table 4).

The relationship between phase II $\dot{V}O_{2p}$ kinetics and [HHb] kinetics was examined by computing the difference in "time to reach steady-state" for both signals (i.e., ($4*\tau\dot{V}O_{2p}$) for $\dot{V}O_{2p}$ and ([HHb]-TD + 4*τ[HHb]) for [HHb], in s) (Figure 8). A "steady-state" for [HHb] was reached ~ 45 s earlier than for $\dot{V}O_{2p}$ for all Δ40W WR transitions (Figure 8A) and ~37 s earlier for WR transitions from a common 20 W baseline (Figure 8B); responses were similar between and within variable and constant baseline conditions ($p>0.05$, Figures 8A and 8B).

The *in silico* simulations using the *in vivo* estimated parameters for $\dot{V}O_{2p}$ kinetics are presented in Figure 9. First, the outcomes from simulations performed to determine values of $\tau\dot{V}O_{2m}$ and $\tau\dot{Q}_m$ that would elicit a $\tau\dot{V}O_{2p}$ of 22 s for the Δ40W step-transition from 20 W were 26.1 s and 28.5 s for $\tau\dot{V}O_{2m}$ and $\tau\dot{Q}_m$, respectively. These values were then used to determine the extent to which $\tau\dot{V}O_{2p}$ would be modified by increasing WR increment (constant baseline condition; Figure 9A) and baseline WR (variable baseline condition; Figure 9B) assuming $\dot{V}O_{2m}$ and $\dot{Q}_m$ kinetics were unaltered. As shown in Figure 9A, the influence on increasing the WR increment in the constant baseline condition is that $\tau\dot{V}O_{2p}$ is reduced from 22.0 s (at Δ40W) to 20.3 s (at Δ100W). The opposite occurs in the variable baseline condition with common Δ40W WR increments, where $\tau\dot{V}O_{2p}$ increases from 22.0 s (at 20 W baseline) to 24.4 s (at 120 W baseline) (Figure 9B). In addition, we also tested the effect of allowing $\dot{Q}_m$ kinetics to become

slower as baseline WR was increased ($\tau\dot{Q}_m$ was increased by 5 s per 20 W increase in baseline). Figure 9C shows that the difference between $\tau\dot{V}O_{2m}$ and $\tau\dot{V}O_{2p}$ tends to become smaller as the baseline WR is increased (variable baseline condition).

Figure 10 displays the results of the simulated six muscle compartment model to a step change from 20 to 120 W. Based on the dynamic responses of $\dot{V}O_{2p}$ and [HHb] from the group means of the equal WR increment steps, the $\dot{V}O_{2m}$ and $\dot{Q}_m$ kinetics for six theoretical muscle compartments were determined: $\tau\dot{V}O_{2m}$ = 15, 20, 25, 30, 35, 40 s and $\tau\dot{Q}_m$ = 20, 25, 30, 35, 40, 45 s (for compartments 1 – 6, respectively). The resultant $\tau\dot{V}O_{2p}$ of the averaged $\dot{V}O_{2p}$ output was 23.5 s, which was less than the mean $\tau\dot{V}O_{2m}$ of all compartments (27.5 s) and very similar to the measured $\dot{V}O_{2p}$ response of 21.8 s (Figure 10).

Discussion

The purpose of this study was to examine the relative stability of phase II $\dot{V}O_{2p}$ and [HHb] kinetics under a wide range of conditions with varying baseline work rate and work rate increment during moderate-intensity exercise. The main findings of the study were that: i) in the variable baseline condition, exercise transitions from a progressively greater baseline WR were associated with progressive increases in both $\tau\dot{V}O_{2p}$ and G_P – the relationships between baseline WR and $\tau\dot{V}O_{2p}$ or G_P were approximately linear; ii) in the constant baseline condition, but with progressively greater ΔWR increments, $\tau\dot{V}O_{2p}$ did not vary, but G_P increased, with increasing WR increment; iii) [HHb] kinetics were consistently faster than $\dot{V}O_{2p}$ kinetics by a magnitude that was essentially constant under all experimental conditions (i.e., a slowing of $\dot{V}O_{2p}$ kinetics was concomitant with a slowing of [HHb] kinetics) suggesting that both $\dot{V}O_{2m}$ and $\dot{Q}_m$ kinetics slowed in concert as baseline work rate increased; and iv) *in silico* simulations of the circulatory influences dissociating $\tau\dot{V}O_{2p}$ from $\tau\dot{V}O_{2m}$ showed that the slowed $\dot{V}O_{2p}$ kinetics observed in the

variable baseline condition were unlikely to be consequent to altered circulatory dynamics. Thus, these data suggest that $\dot{V}O_{2p}$ kinetics may be dependent on the instantaneous metabolic rate from which they are initiated. However, the *in silico* simulations suggest that metabolic and circulatory dynamics can turn a heterogeneous (or summed) $\dot{V}O_{2m}$ response containing kinetically slow compartments into a uniformly fast $\dot{V}O_{2p}$ response. Therefore, we propose that intracellular O_2 utilization dynamics are first order and are intrinsically slower (in a progressive manner) in muscle fibres located at higher positions within the fibre recruitment hierarchy.

Mechanisms of $\dot{V}O_2$ kinetic control

Intriguingly, our finding that $\dot{V}O_{2p}$ kinetics were constant during different WR increments initiated from a common baseline (20 W) is consistent with the traditional suggestion that a first order rate reaction controls $\dot{V}O_{2p}$ kinetics (Whipp & Mahler, 1980; Barstow & Mole, 1991; Özyener *et al.* 2001; Scheuermann & Barstow, 2003; Spencer *et al.* 2013). However, the finding that $\dot{V}O_{2p}$ kinetics increased linearly with increasing baseline work rate is also consistent with the frequent and long-standing observation that moderate-intensity $\dot{V}O_{2p}$ kinetics are not first order (Hughson & Morrissey, 1982; Brittain *et al.* 2001; Robergs, 2014). Importantly, these findings were made within the same group of participants, ruling-out individual participant differences as an explanation for differences when comparing amongst published studies.

When two identical step-WR increments (between 20 W and 90% $\hat{\theta}_L$) bisecting the moderate-intensity domain are performed, the kinetics of $\dot{V}O_{2p}$ are consistently slower in the upper compared to the lower step-transition (Brittain *et al.* 2001; MacPhee *et al.* 2005; Bowen *et al.* 2011; Williams *et al.* 2013; Keir *et al.* 2014). By examining a range of pre-transition baseline work and metabolic rates spanning the entire moderate-intensity domain, the present study extends previous findings to show that both $\tau\dot{V}O_{2p}$ and G_P increase as a function of pre-transition

baseline WR and metabolic rate in an approximately linear manner. This phenomenon has been previously explained by two hypotheses. The first is a fibre activation pattern favouring "kinetically-faster", more efficient fibres, to perform lower intensities and a progressive incorporation of "kinetically-slower" fibres to perform greater external WRs (Brittain *et al.* 2001). An alternative view proposes that $\dot{V}O_{2p}$ kinetics are influenced by the pre-transition metabolic rate such that greater reductions in intracellular energy state cause less free energy delivery from the mitochondria and increase the demand for mitochondrial ATP production (Bowen *et al.* 2011; Wüst *et al.* 2014). It currently is not possible to know whether the muscle motor units recruited to transition to low work rates are the same or different from those recruited to transition to greater work rates. Thus, we cannot distinguish whether the present results are due to recruitment of motor units innervating muscle fibres with inherently different mitochondrial volume-density, or whether our findings were consequent to a progressive contribution of increasing metabolic rate within a uniform fibre population.

It has been suggested that the free energy associated with ATP hydrolysis (ΔG_{ATP}, i.e., ~58 kJ·mol^{-1}) is greater than the activation energy required for acto-myosin crossbridge cycling (~ 40 kJ·mol^{-1} (Sheetz *et al.* 1984) but close to that for SERCA ATPase function (~ 52 kJ·mol^{-1}) under normal physiological conditions (Grassi *et al.* 2015). Since the concentration of metabolites that affect ΔG_{ATP} (i.e., [ADP_{free}] and [Pi]) are elevated at greater baseline metabolic rates, less negative ΔG_{ATP} could prevent some acto-myosin crossbridge or SERCA ATPase regions from receiving sufficient energy to activate. The resultant effect would be a progressively larger and possibly less "square wave" change in ATP required for a given change in WR, thereby altering the exponential-nature of the response leading to an increase in both $\tau\dot{V}O_{2p}$ and G_P. However, this hypothesis is difficult to reconcile in moderate-intensity cycling

exercise, where muscle fatigue appears to be absent (Cannon *et al.* 2011). An alternative mechanism could be that $\dot{V}O_{2m}$ of individual fibers does operate through a unimolecular reaction of ADP-feedback to its mitochondrial network; when these same fibers are recruited at a greater level of metabolic activity, the intracellular [ADP_{free}] exceeds the K_m and thus the sensitivity of $\dot{V}O_{2m}$ to increases in [ADP_{free}] may decrease, manifesting as a slower rate of adjustment in $\dot{V}O_{2p}$ with a greater baseline metabolic rate. Nevertheless, this also seems unlikely in moderate exercise where intramyocellular disturbance in [ADP_{free}] in the active fibres is likely small and thus an alternative explanation is required.

In silico simulations

Using *in silico* simulations based on a validated multi-compartmental model of circulatory dynamics, Benson *et al.* (2013) demonstrated that kinetic dissociations between phase II $\dot{V}O_{2p}$ and $\dot{V}O_{2m}$ can occur dependent on both the dynamics of muscle and whole body $\dot{Q}$ and flow-weighted mixing of muscle and whole body venous effluents. In the present study, this model was applied to assess whether altered circulatory dynamics with transitions from increasing baseline WRs might distort, by "slowing", the dynamic adjustment of the $\dot{V}O_{2p}$ profile despite $\dot{V}O_{2m}$ kinetics being "constant" when transitioning from progressively higher starting baseline metabolic rates. When assuming constant kinetics for $\dot{V}O_{2m}$ ($\tau\dot{V}O_{2m}$, 26.1 s) and $\dot{Q}_m$ (28.5 s) (see Methods), simulations showed that constant Δ40W step-transitions initiated from progressively higher baseline WRs (from 20 to 120W) were associated with a slight ~ 2 s increase in $\tau\dot{V}O_{2p}$ (22.0 to 24.2 s); however, this effect was not large enough to explain the observed $\tau\dot{V}O_{2p}$ which increased from 22 s to 35 s under the same conditions. This suggests that significant "distortion" of the $\dot{V}O_{2m}$ profile at the lung because of circulatory dynamics and mixing of muscle and other body venous compartments, while potentially contributory, likely

were not responsible for the major progressive slowing of $\dot{V}O_{2p}$ kinetics observed in this study (Bowen *et al.* 2011).

That [HHb] kinetics were consistently faster than $\dot{V}O_{2p}$ kinetics suggests that, overall, during the on-transient phase, a greater rate of O_2 extraction was required relative to the rate of muscle O_2 utilization. Since, the magnitude by which kinetics of both signals differed did not change as a function of baseline WR (Figure 8) suggests that the underlying microvascular blood flow ($\dot{Q}_m$) dynamics were slightly slower than $\dot{V}O_{2m}$ and that $\dot{Q}_m$ became progressively slower with transitions from greater baseline WRs. Given that MacPhee *et al.* (2005) also reported a twofold increase in the time constant for bulk leg blood flow when equal WR increment step-transitions were initiated from WRs midway between 20W and 90% $\hat{\theta}_L$ compared to a baseline of 20W, we examined the effect of progressively increasing $\tau\dot{Q}_m$ (by a factor of ~5 s per 20W increase in baseline; MacPhee *et al.* (2005)) on the modulation of $\tau\dot{V}O_{2p}$ for a range of $\tau\dot{V}O_{2m}$ (from 20 – 40 s; Figure 9C). For any given $\tau\dot{V}O_{2m}$, $\tau\dot{V}O_{2p}$ was reduced as baseline WR and $\tau\dot{Q}_m$ increased (a relationship opposite to that observed experimentally in the present study). This further supports the notion that the slowing of $\dot{V}O_{2p}$ kinetics coincident with higher baseline metabolic rates, seen in this and other studies, reflects an actual slowing of $\dot{V}O_{2m}$ kinetics, and is not a consequence of circulatory-induced "distortions" of an unchanging $\dot{V}O_{2m}$ profile.

Since It has been suggested that the dynamics of O_2 delivery are regionally heterogeneous within human quadriceps muscle (Koga *et al.* 2007), we further used this model to provide an additional explanation to reconcile why $\dot{V}O_{2p}$ kinetics were slowed (from ~ 22 s to ~ 35 s) in transitions initiated from progressively higher baseline WRs but are fast (~ 20 s) and unchanged with transitions initiated from a 20 W baseline but increasing ΔWR increment. In accordance with Koga *et al.* (2007), we proposed that "kinetically-faster" fibre pools

446 (presumably those with a greater mitochondrial volume and better blood supply) dominate the
447 collective, or homogenized, $\dot{V}O_{2p}$ response by exerting a greater influence on C_vO_2 of the blood
448 draining the muscle during the early portion of the transition. To explore this suggestion we used
449 a model broadly based on the six muscle "compartments" derived from the responses to the six
450 □40W steps that were examined in this study. We assumed that each compartment was of equal
451 size but varied in $\dot{V}O_{2m}$ and $\dot{Q}_m$ kinetics. We examined the average $\dot{V}O_{2p}$ response to a step-
452 change in WR from 20 to 120 W derived from the simultaneous activation of these
453 compartments (see Methods). $\dot{V}O_{2m}$ and $\dot{Q}_m$ kinetics for each compartment were determined *ad-*
454 *hoc* and were selected to reflect the kinetics (as inferred from $\dot{V}O_{2p}$ and [HHb]) from the group
455 means of the equal WR increment steps ($\tau\dot{V}O_{2m}$ = 15, 20, 25, 30, 35, 40 s and $\tau\dot{Q}_m$ = 20, 25, 30,
456 35, 40, 45 s for compartments 1 – 6, respectively). There was a slight discrepancy between the
457 $\dot{V}O_{2p}$ model output and the measured $\dot{V}O_{2p}$ response (Figure 10) in the early phase (phase I) of
458 the transition (possibly due to differences in the blood flow profile during abrupt transitions from
459 Δ100W compared to Δ40W). However, phase II $\tau\dot{V}O_{2p}$ was 23.5 s which was less than the mean
460 $\tau\dot{V}O_{2m}$ of all compartments (27.5 s) and very similar to the measured $\dot{V}O_{2p}$ response of 22 s. This
461 suggests that the conflation of $\dot{Q}_m$ dynamics amongst compartments may modulate the
462 "summated" $\dot{V}O_{2m}$ kinetics towards a faster $\tau\dot{V}O_{2p}$ via disproportionate and time-dependent
463 contributions (of those compartments) to the dynamics of C_vO_2 of blood draining the muscle.
464 Therefore, it is possible that the $\tau\dot{V}O_{2p}$ from the larger step-changes (i.e., greater WR increments)
465 may have been influenced by the blood flow and metabolic heterogeneity and differences in
466 circulatory and metabolic dynamics existing within the pool of muscle fibres recruited to support
467 the change in WR. Although $\dot{Q}_m$ dynamics were not directly measured, microvascular O_2
468 pressure ($P_{mv}O_2$) has been shown to drop at a faster rate and to a greater extent at the onset of

contraction in rat muscle comprised predominately of fast- compared to slow-muscle fibres (Behnke *et al.* 2003; McDonough *et al.* 2005). Therefore, it is conceivable that human skeletal muscle may also express diversity in $\dot{Q}_m$ dynamics such that muscle fibres with slow $\dot{V}O_{2m}$ kinetics may also have slower blood flow dynamics.

Reconciling models of $\dot{V}O_{2p}$ kinetic control

Thus, while distinguishing among the various hypotheses for $\dot{V}O_{2p}$ kinetic control will require complex and detailed descriptions of $\dot{V}O_{2m}$ and intramyocellular signalling dynamics under a range of conditions (such as those used in this study), our combined *in vivo* and *in silico* data propose a unifying hypothesis. That $\dot{V}O_{2p}$ kinetics were invariant in the moderate domain with constant baseline WR is consistent with first order control. While the progressive increase in $\tau\dot{V}O_{2p}$ with increasing baseline work rates appears to subvert the requirements of a first order system, we propose that these findings can be reconciled by the understanding of the heterogeneity in both dynamics of muscle motor unit recruitment (of fibres with different a volume of mitochondrial network) and of blood flow (where the microvascular blood flow dynamics may vary to a similar magnitude to $\dot{V}O_{2p}$ kinetics). Thus, the transit and mixing of blood draining kinetically variable motor units are later combined to form a $\dot{V}O_{2p}$ kinetic response that is dominated by the influence of the motor units where both $\dot{V}O_{2m}$ and $\dot{Q}_m$ kinetics are fast. These features can explain both the main findings of $\dot{V}O_{2p}$ kinetic behaviour in this study and remain consistent with the assumptions of apparent first order control.

Conclusion

The main finding of the present study was that $\dot{V}O_{2p}$ kinetics are not altered when step-changes are initiated from a 20 W baseline WR, but get progressively slower with increasing baseline work rate. The observed slowing of $\dot{V}O_{2p}$ kinetics with increasing baseline intensity

could not be attributed to limitations in O_2 delivery (since the magnitude of the difference between kinetic adjustments of [HHb] and $\dot{V}O_{2p}$ was unchanged regardless of baseline WR or ΔWR increment). However, a model combining heterogeneous metabolism and blood flow kinetics was able to reconcile these apparently conflicting findings. Collectively, these data suggest that within the moderate-intensity domain phase II $\dot{V}O_{2p}$ kinetics are influenced by pre-transition WR, becoming slower as baseline WR increases, and are strongly influenced by heterogeneity in the dynamic metabolic and circulatory properties of the active muscles. Taken together, these data suggest that the work rate-dependent non-linear $\dot{V}O_{2p}$ responses may be attributable to "heterogeneity" within the range of muscle fibres recruited to address the exercise challenge. Importantly, each of these muscle fibres may independently behave as a linear, first order system.

Acknowledgments: We would like to express our gratitude to the participants in this study. We also extend our gratitude to Professor P.A. Robbins, University of Oxford, for providing the "End-tidal Forcing" software for breath-by-breath pulmonary oxygen uptake measurement.

Grants: This study was supported by the National Science and Engineering Research Council of Canada (NSERC) research and equipment grants (RGPGP-2015-00084). Daniel A. Keir was supported by a Post-Graduate Doctoral Scholarship from NSERC.

Disclosures: No conflicts of interest, financial or otherwise, are declared by the authors.

Author Contributions: D.A.K and J.M.K. conceived and designed the study; D.A.K and T.C.R collected the data; A.P.B collected the computational data; all authors interpreted the results of the experiment/simulations; D.A.K. prepared the figures and the first draft of the manuscript; all authors edited and approved the final version of the manuscript.

References

Barstow TJ, Lamarra N & Whipp BJ (1990). Modulation of muscle and pulmonary O_2 uptakes by circulatory dynamics during exercise. *J Appl Physiol* **68,** 979–989.

Barstow TJ & Mole PA (1991). Linear and nonlinear characteristics of oxygen uptake kinetics during heavy exercise. *J Appl Physiol* **71,** 2099–2106.

Beaver WL, Wasserman K & Whipp BJ (1986). A new method for detecting anaerobic threshold by gas exchange. *J Appl Physiol* **60,** 2020–2027.

Behnke BJ, McDonough P, Padilla DJ, Musch TI & Poole DC (2003). Oxygen exchange profile in rat muscles of contrasting fibre types. *J Physiol* **549,** 597–605.

Benson AP, Grassi B & Rossiter HB (2013). A validated model of oxygen uptake and circulatory dynamic interactions at exercise onset in humans. *J Appl Physiol* **115,** 743–755.

Bowen TS, Murgatroyd SR, Cannon DT, Cuff TJ, Lainey AF, Marjerrison AD, Spencer MD, Benson AP, Paterson DH, Kowalchuk JM & Rossiter HB (2011). A raised metabolic rate slows pulmonary O_2 uptake kinetics on transition to moderate-intensity exercise in humans independently of work rate. *Exp Physiol* **96,** 1049–1061.

Brittain CJ, Rossiter HB, Kowalchuk JM & Whipp BJ (2001). Effect of prior metabolic rate on the kinetics of oxygen uptake during moderate-intensity exercise. *Eur J Appl Physiol* **86,** 125–134.

Cannon DT, White AC, Andriano MF, Kolkhorst FW & Rossiter HB (2011). Skeletal muscle fatigue precedes the slow component of oxygen uptake kinetics during exercise in humans. *J Physiol* **589,** 727–739.

DiMenna FJ, Bailey SJ, Vanhatalo A, Chidnok W & Jones AM (2010). Elevated baseline VO_2 per se does not slow O_2 uptake kinetics during work-to-work exercise transitions. *J Appl Physiol* **109,** 1148–1154.

Grassi B, Poole DC, Richardson RS, Knight DR, Erickson BK & Wagner PD (1996). Muscle O_2 uptake kinetics in humans: implications for metabolic control. *J Appl Physiol* **80,** 988–998.

Grassi B, Rossiter HB & Zoladz JA (2015). Skeletal muscle fatigue and decreased efficiency: two sides of the same coin? *Exerc Sport Sci Rev* **43,** 75–83.

Hoffmann U, Drescher U, Benson AP, Rossiter HB & Essfeld D (2013). Skeletal muscle VO_2 kinetics from cardio-pulmonary measurements: assessing distortions through O_2 transport by means of stochastic work-rate signals and circulatory modelling. *Eur J Appl Physiol* **113,** 1745–1754.

Hughson RL & Morrissey M (1982). Delayed kinetics of respiratory gas exchange in the transition from prior exercise. *J Appl Physiol* **52,** 921–929.

Keir DA, Nederveen JP, Paterson DH & Kowalchuk JM (2014). Pulmonary O_2 uptake kinetics during moderate-intensity exercise transitions initiated from low versus elevated metabolic rates: insights from manipulations in cadence. *Eur J Appl Physiol* **114,** 2655–2665.

Koga S, Poole DC, Ferreira LF, Whipp BJ, Kondo N, Saitoh T, Ohmae E & Barstow TJ (2007). Spatial heterogeneity of quadriceps muscle deoxygenation kinetics during cycle exercise. *J Appl Physiol (Bethesda, Md 1985)* **103,** 2049–2056.

Krustrup P, Jones AM, Wilkerson DP, Calbet JAL & Bangsbo J (2009). Muscular and pulmonary O_2 uptake kinetics during moderate- and high-intensity sub-maximal knee-extensor exercise in humans. *J Physiol* **587,** 1843–1856.

Lamarra N, Whipp BJ, Ward SA & Wasserman K (1987). Effect of interbreath fluctuations on characterizing exercise gas exchange kinetics. *J Appl Physiol* **62,** 2003–2012.

MacPhee SL, Shoemaker JK, Paterson DH & Kowalchuk JM (2005). Kinetics of O_2 uptake, leg blood flow, and muscle deoxygenation are slowed in the upper compared with lower region of the moderate-intensity exercise domain. *J Appl Physiol* **99,** 1822–1834.

McDonough P, Behnke BJ, Padilla DJ, Musch TI & Poole DC (2005). Control of microvascular oxygen pressures in rat muscles comprised of different fibre types. *J Physiol* **563,** 903–913.

Murias JM, Spencer MD & Paterson DH (2014). The critical role of O_2 provision in the dynamic adjustment of oxidative phosphorylation. *Exerc Sport Sci Rev* **42,** 4–11.

Özyener F, Rossiter HB, Ward SA & Whipp BJ (2001). Influence of exercise intensity on the on- and off-transient kinetics of pulmonary oxygen uptake in humans. *J Physiol* **533,** 891–902.

Robergs RA (2014). A critical review of the history of low- to moderate-intensity steady-state VO_2 kinetics. *Sport Med* **44,** 641–653.

Rossiter HB (2011). Exercise: Kinetic Considerations for Gas Exchange. *Compr Physiol* **1,** 203–244.

Scheuermann BW & Barstow TJ (2003). O_2 uptake kinetics during exercise at peak O_2 uptake. *J Appl Physiol* **95,** 2014–2022.

Sheetz MP, Chasan R & Spudich J a. (1984). ATP-dependent movement of myosin in vitro: Characterization of a quantitative assay. *J Cell Biol* **99,** 1867–1871.

Spencer MD, Murias JM, Kowalchuk JM & Paterson DH (2011). Pulmonary O_2 uptake and muscle deoxygenation kinetics are slowed in the upper compared with lower region of the moderate-intensity exercise domain in older men. *Eur J Appl Physiol* **111,** 2139–2148.

Spencer MD, Murias JM, Kowalchuk JM & Paterson DH (2013). Effect of moderate-intensity work rate increment on phase II tauVO_2, functional gain and Delta[HHb]. *Eur J Appl Physiol* **113,** 545–557.

Spencer MD, Murias JM & Paterson DH (2012). Characterizing the profile of muscle deoxygenation during ramp incremental exercise in young men. *Eur J Appl Physiol* **112,** 3349–3360.

Swanson GD (1980). Breath-to-breath considerations for gas exchange kinetics. In *Exercise Bioenergetics and Gas Exchange*, ed. Cerretelli P & Whipp BJ, pp. 211–222. Elsevier, Amsterdam.

Whipp BJ & Mahler M (1980). Dynamics of pulmonary gas exchange during exercise. In *Pulmonary Gas Exchange, Vol II, Organism and Environment*, ed. West JB, pp. 33–96. Academic Press, New York.

Whipp BJ, Ward SA, Lamarra N, Davis JA & Wasserman K (1982). Parameters of ventilatory and gas exchange dynamics during exercise. *J Appl Physiol* **52,** 1506–1513.

Williams AM, Paterson DH & Kowalchuk JM (2013). High-intensity interval training speeds the adjustment of pulmonary O_2 uptake, but not muscle deoxygenation, during moderate-intensity exercise transitions initiated from low and elevated baseline metabolic rates. *J Appl Physiol* **114,** 1550–1562.

Wüst RC, McDonald JR, Sun Y, Ferguson BS, Rogatzki MJ, Spires J, Kowalchuk JM, Gladden LB & Rossiter HB (2014). Slowed muscle oxygen uptake kinetics with raised metabolism are not dependent on blood flow or recruitment dynamics. *J Physiol* **592,** 1857–1871.

Wüst RCI, Grassi B, Hogan MC, Howlett R a, Gladden LB & Rossiter HB (2011). Kinetic control of oxygen consumption during contractions in self-perfused skeletal muscle. *J Physiol* **589,** 3995–4009.

608 **Table Legends**

609 **Table 1.** Mean parameter estimates and fit statistics of phase II $\dot{V}O_{2p}$ data for each 40W
610 transition from progressively increasing baseline work rates (mean ± SD)

611 [a-f] indicate significant differences between conditions ($p<0.05$). "[a]" indicates difference from "**20**
612 **→ 60**", "[b]" indicates difference from "**40 → 80**", and so forth. * indicates significant differences
613 amongst all conditions ($p<0.05$).

614

615 **Table 2.** Mean parameter estimates and fit statistics of phase II $\dot{V}O_{2p}$ data for each ΔWR
616 transition from a constant baseline of 20W (mean ± SD)

617 [a-d] indicate significant differences between conditions ($p<0.05$). "[a]" indicates difference from "**20**
618 **→ 60**", "[b]" indicates difference from "**20 → 80**", and so forth. * indicates significant differences
619 amongst all conditions ($p<0.05$).

620

621 **Table 3.** Mean parameter estimates and confidence interval of mono-exponential fit of [HHb]
622 data for each 40W transition from progressively increasing baseline work rates (mean ± SD)

623 [a-f] indicate significant differences between conditions ($p<0.05$). "[a]" indicates difference from "**20**
624 **→ 60**", "[b]" indicates difference from "**40 → 80**", and so forth. * indicates significant differences
625 amongst all conditions ($p<0.05$).

626

627 **Table 4.** Mean parameter estimates and confidence interval of mono-exponential fit of [HHb]
628 data for each ΔWR transition from a constant baseline of 20W (mean ± SD)

629 [a-d] indicate significant differences between conditions ($p<0.05$). "[a]" indicates difference from "**20**

630 **→ 60**", "[b]" indicates difference from "**20 → 80**", and so forth. ***** indicates significant differences

631 amongst all conditions ($p<0.05$).

632

633 **Figure Captions**

634 **Figure 1.** Schematic of experimental protocols and procedures. See text for details.

635

636 **Figure 2.** Ensemble-averaged group mean responses of $\dot{V}O_{2p}$ in the variable baseline condition:
637 six 40 W transitions from different baseline work rates. Vertical dashed lines indicate the onset
638 of the transition (time = 0 s). The group mean phase II kinetic responses for each condition are
639 superimposed on the data (*dark lines*, fitted with a mono-exponential function using group mean
640 parameter estimates). $\tau\dot{V}O_{2p}$ values (± SD) are inset under each transition and error bars at
641 specific time points indicate SD.

642

643 **Figure 3.** A) Baseline $\dot{V}O_{2p}$ ($\dot{V}O_{2pBSL}$) as a function of baseline WR. B) $\dot{V}O_{2p}$ amplitude (A) as
644 function of $\dot{V}O_{2pBSL}$. C) $\dot{V}O_{2p}$ time constant ($\tau\dot{V}O_{2p}$) as function of $\dot{V}O_{2pBSL}$. D) Gain (G_P) as
645 function of $\dot{V}O_{2pBSL}$. Symbols represent group mean ± SD. [a-f] indicate significant differences
646 between conditions ($p<0.05$). "[a]" indicates difference from "**20 → 60**", "[b]" indicates difference
647 from "**40 → 80**", and so forth. * indicates significant differences amongst all transitions
648 ($p<0.05$).

649

650 **Figure 4.** Ensemble-averaged group mean responses of $\dot{V}O_{2p}$ in the constant baseline condition:
651 four different increments in work rate (ΔWR) each from a 20 W baseline work rate. Vertical
652 dashed lines indicate the onset of the transition (time = 0 s). The group mean phase II kinetic
653 responses for each condition are superimposed over the data (*dark lines*, fitted with a mono-
654 exponential function using group mean parameter estimates). $\tau\dot{V}O_{2p}$ values (± SD) are inset
655 under each transition and error bars at specific time points indicate SD.

Figure 5. Comparison of A) baseline $\dot{V}O_{2p}$ ($\dot{V}O_{2pBSL}$); B) $\dot{V}O_{2p}$ amplitude (A); C) $\dot{V}O_{2p}$ time constant ($\tau\dot{V}O_{2p}$); and D) gain (G_P) as function of as a function of WR increment (ΔWR). Symbols represent group mean ± SD. [a-d] indicate significant differences between conditions ($p<0.05$). "[a]" indicates difference from "**20 → 60**", "[b]" indicates difference from "**20 → 80**", and so forth.* indicates significant differences amongst all transitions ($p<0.05$).

Figure 6. Ensemble-averaged group mean responses of [HHb] in the variable baseline condition: six 40 W transitions from different baseline work rates. Vertical dashed lines indicate the onset of the transition (time = 0 s). The group mean phase II kinetic responses for each condition are superimposed on the data (*dark lines*, fitted with a mono-exponential function using group mean parameter estimates). τ[HHb] values (± SD) are inset under each transition and error bars at specific time points indicate SD. Error bars at specific time points are not displayed due to the large SD in [HHb] amongst subjects (see Table 3).

Figure 7. Ensemble-averaged group mean responses of [HHb] in the constant baseline condition: four different increments in work rate (ΔWR) each from a 20 W baseline work rate. Vertical dashed lines indicate the onset of the transition (time = 0 s). The group mean phase II kinetic responses for each condition are superimposed over the data (*dark lines*, fitted with a mono-exponential function using group mean parameter estimates). τ[HHb] values (± SD) are inset under each transition. Error bars at specific time points are not displayed due to the large SD in [HHb] amongst subjects (see Table 4).

679

680

681 **Figure 8.** Comparison of the "time to reach steady-state" between $\dot{V}O_{2p}$ and NIRS-derived
682 deoxygenated hemoglobin ([HHb]) signals following exercise onset. "Time to reach steady-
683 state" was computed as the difference between the sum of 4 time constants for phase II $\dot{V}O_{2p}$ (4 x
684 $\tau\dot{V}O_{2p}$) and 4 time constants plus the time delay for [HHb] ([HHb]-TD + (4 x τ[HHb])). Panel *A*
685 shows group mean ± SD for the variable baseline condition; 40 W transitions from different
686 baseline work rates (*black bars*). Panel *B* shows group mean ± SD for each the constant baseline
687 condition; variable increments in work rate each from a 20 W baseline (*grey bar*). There were no
688 differences amongst transitions ($p>0.05$).

689

690 **Figure 9.** The output of a dynamic computational simulation to illustrate the influence of
691 circulatory dynamics on the phase II pulmonary $\dot{V}O_{2p}$ during exercise transitions in both the
692 variable and constant baseline conditions. Modulation of $\tau\dot{V}O_{2p}$ at a fixed muscle $\tau\dot{V}O_2$ ($\tau\dot{V}O_{2m}$;
693 26.1 s) and muscle $\tau\dot{Q}$ ($\tau\dot{Q}_m$; 28.5 s) is examined for step-transitions from a 20 W baseline to
694 increasing ΔWR increments (*panel A*) and for Δ40W step-transitions from increasing baseline
695 WR (WR_{bsl}; *panel B*). *Panel C* displays the effect of circulatory dynamics on $\tau\dot{V}O_{2p}$ during
696 simulated Δ40W exercise transitions from increasing baseline WRs at various $\tau\dot{V}O_{2m}$ (*circles*, 20
697 s; *triangles*, 30 s; *squares*, 40 s). The $\tau\dot{Q}_m$ values used in the simulations are based on data from
698 MacPhee et al. (2005) who showed that $\dot{Q}_m$ dynamics slow with transitions from elevated
699 metabolic rates. Note that as $\tau\dot{Q}_m$ increases with increasing baseline WR for each isopleth of
700 $\tau\dot{V}O_{2m}$, $\tau\dot{V}O_{2p}$ becomes smaller (faster kinetics) which is opposite to the results from the *in vivo*
701 data. See text for further explanation.

Figure 10. Ensemble-averaged group mean responses of $\dot{V}O_{2p}$ for the Δ100W step-transition from a 20 W baseline work rate. Vertical dashed lines indicate the onset of the transition (time = 0 s). A theoretical model containing six muscle compartments of equal size but varying $\dot{V}O_{2m}$ and $\dot{Q}_m$ kinetics ($\tau\dot{V}O_{2m}$ = 15, 20, 25, 30, 35, 40 s and $\tau\dot{Q}_m$ = 20, 25, 30, 35, 40, 45 s for compartments 1 – 6, respectively) was developed and computational simulations were used to investigate whether the conflation of $\dot{Q}_m$ dynamics amongst compartments may modulate the "summed" (or homogenized) $\dot{V}O_{2m}$ kinetics towards a faster $\tau\dot{V}O_{2p}$ response in a 100W step-change from 20 W. Assuming equal contributions from each compartment, the resultant $\dot{V}O_{2p}$ response (*black line*) is overlaid on the *in vivo* group mean response (*white circles*). The phase II $\tau\dot{V}O_{2p}$ from the six compartment model was 23.5 s, which is slightly faster than the mean $\tau\dot{V}O_{2m}$ of all compartments, 27.5 s and similar to the $\tau\dot{V}O_{2p}$ measured in the study participants (21.8 ± 4.8 s).

Table 1. Mean parameter estimates (± SD) for phase II $\dot{V}O_{2p}$ kinetics during 40 W exercise transitions from six different baseline work rates (variable baseline condition).

	Step-transition power output (W)					
n = 14	**20 → 60**	**40 → 80**	**60 → 100**	**80 → 120**	**100 → 140**	**120 → 160**
$\dot{V}O_{2pBSL}$ ($L \cdot min^{-1}$)*	0.75 ± 0.07	0.93 ± 0.06	1.10 ± 0.07	1.30 ± 0.06	1.48 ± 0.06	1.71 ± 0.08
A ($L \cdot min^{-1}$)	0.35 ± 0.02^{cdef}	0.37 ± 0.02^{def}	0.39 ± 0.02^{af}	0.40 ± 0.20^{ab}	0.41 ± 0.03^{ab}	0.42 ± 0.04^{abc}
$\dot{V}O_{2pSS}$ ($L \cdot min^{-1}$)*	1.10 ± 0.07	1.30 ± 0.06	1.49 ± 0.07	1.70 ± 0.07	1.90 ± 0.07	2.12 ± 0.08
TD (s)	12 ± 6	10 ± 4	7 ± 6	6 ± 6	6 ± 3	7 ± 3
$\tau\dot{V}O_{2p}$ (s)	22 ± 5^{cdef}	23 ± 5^{def}	28 ± 6^{af}	31 ± 7^{ab}	34 ± 6^{ab}	35 ± 9^{abc}
CI_{95} (s)	3 ± 1	3 ± 1	3 ± 1	4 ± 1	4 ± 1	4 ± 1
χ^2 (x 10^{-4})	7.6 ± 4.2	10.2 ± 5.8	8.9 ± 3.8	12.2 ± 5.7	11.3 ± 4.5	13.6 ± 4.4
MRT-$\dot{V}O_{2p}$ (s)	34 ± 6^{ef}	32 ± 4^{ef}	36 ± 7^{f}	38 ± 6	41 ± 6^{ab}	45 ± 13^{abc}
O_{2Def} (mL)	193 ± 32^{def}	197 ± 26^{ef}	233 ± 43^{f}	251 ± 47^{af}	285 ± 51^{ab}	319 ± 115^{abcd}
G_P ($mL \cdot min^{-1} \cdot W^{-1}$)	8.7 ± 0.6^{cdef}	9.2 ± 0.5^{def}	9.7 ± 0.6^{af}	10.0 ± 0.6^{ab}	10.3 ± 0.8^{ab}	10.5 ± 0.9^{abc}

$^{a\text{-}f}$ indicate significant differences between conditions ($p<0.05$). "^{a}" indicates difference from "**20 → 60**", "^{b}" indicates difference from "**40 → 80**", and so forth. * indicates significant differences amongst all conditions ($p<0.05$).

Table 2. Mean parameter estimates (± SD) for phase II $\dot{V}O_{2p}$ kinetics during exercise transitions from 20W to four different work rates (constant baseline condition).

	Step-transition power output (W)			
n = 14	**20 → 60**	**20 → 80**	**20 → 100**	**20 → 120**
$\dot{V}O_{2pBSL}$ ($L \cdot min^{-1}$)	0.75 ± 0.07	0.75 ± 0.06	0.76 ± 0.06	0.76 ± 0.06
A ($L \cdot min^{-1}$)*	0.35 ± 0.02	0.54 ± 0.02	0.72 ± 0.04	0.93 ± 0.04
$\dot{V}O_{2pSS}$ ($L \cdot min^{-1}$)*	1.10 ± 0.07	1.30 ± 0.06	1.47 ± 0.05	1.68 ± 0.07
TD (s)	12 ± 6	11 ± 4	12 ± 3	11 ± 3
$\tau\dot{V}O_{2p}$ (s)	22 ± 5	20 ± 4	22 ± 6	22 ± 5
CI_{95} (s)	3 ± 1	2 ± 1	2 ± 1	1 ± 0
χ^2 (x 10^{-4})	7.6 ± 4.2	10.7 ± 5.3	12.0 ± 5.5	12.5 ± 4.5
MRT-$\dot{V}O_{2p}$ (s)	34 ± 6	31 ± 3	33 ± 4	33 ± 5
O_{2Def} (mL)*	193 ± 32	276 ± 26	389 ± 47	501 ± 73
G_P ($mL \cdot min^{-1} \cdot W^{-1}$)	8.7 ± 0.6[bd]	9.0 ± 0.4[a]	8.9 ± 0.4	9.3 ± 0.4[a]

[a-d] indicate significant differences between conditions ($p<0.05$). "[a]" indicates difference from "**20 → 60**", "[b]" indicates difference from "**20 → 80**", and so forth. * indicates significant differences amongst all conditions ($p<0.05$).

Table 3. Mean parameter estimates and confidence interval of mono-exponential fit of [HHb] data for each 40W transition from progressively increasing baseline work rates (mean ± SD)

	Step-transition power output (W)					
	20 → 60	**40 → 80**	**60 → 100**	**80 → 120**	**100 → 140**	**120 → 160**
$[HHb]_{bsl}$ (μM) *	19.2 ± 7.2	21.9 ± 8.1	22.3 ± 8.9	24.0 ± 9.5	24.5 ± 10.6	27.1 ± 11.5
$\Delta[HHb]_{amp}$ (μM)	3.4 ± 2.6	2.6 ± 1.4	2.6 ± 2.1	3.1 ± 2.8	2.7 ± 2.2	3.0 ± 2.5
[HHb]-TD (s)	16 ± 4[ef]	15 ± 3[e]	13 ± 4	11 ± 5	11 ± 4[a]	9 ± 5[ab]
τ[HHb] (s)	9 ± 4[def]	11 ± 3	14 ± 7	17 ± 6[a]	18 ± 11[a]	18 ± 6[a]
MRT-[HHb] (s)	25 ± 6	26 ± 5	26 ± 6	28 ± 5	29 ± 9	28 ± 5
CI_{95} (s)	1 ± 1	2 ± 1	2 ± 1	2 ± 1	2 ± 1	2 ± 1

[a-f] indicate significant differences between conditions ($p<0.05$). "[a]" indicates difference from "**20 → 60**", "[b]" indicates difference from "**40 → 80**", and so forth. * indicates significant differences amongst all conditions ($p<0.05$).

Table 4. Mean parameter estimates and confidence interval of mono-exponential fit of [HHb] data for each ΔWR transition from a constant baseline of 20W (mean ± SD)

	Step-transition power output (W)			
	20 → 60	**20 → 80**	**20 → 100**	**20 → 120**
$[HHb]_{bsl}$ (μM)	19.2 ± 7.2	19.8 ± 7.1	19.2 ± 7.2	19.9 ± 7.6
$\Delta[HHb]_{amp}$ (μM)	3.4 ± 2.6 *	4.8 ± 3.3 *	6.3 ± 4.6 *	9.4 ± 2.8 *
[HHb]-TD (s)	16 ± 4	14 ± 3	13 ± 2	11 ± 3
τ[HHb] (s)	9 ± 4	10 ± 5	8 ± 3	8 ± 3
MRT-[HHb] (s)	25 ± 6	24 ± 7	20 ± 4	20 ± 4
CI_{95} (s)	1 ± 1	1 ± 1	1 ± 1	1 ± 0

[a-d] indicate significant differences between conditions ($p<0.05$). "[a]" indicates difference from "**20 → 60**", "[b]" indicates difference from "**20 → 80**", and so forth. * indicates significant differences amongst all conditions ($p<0.05$).

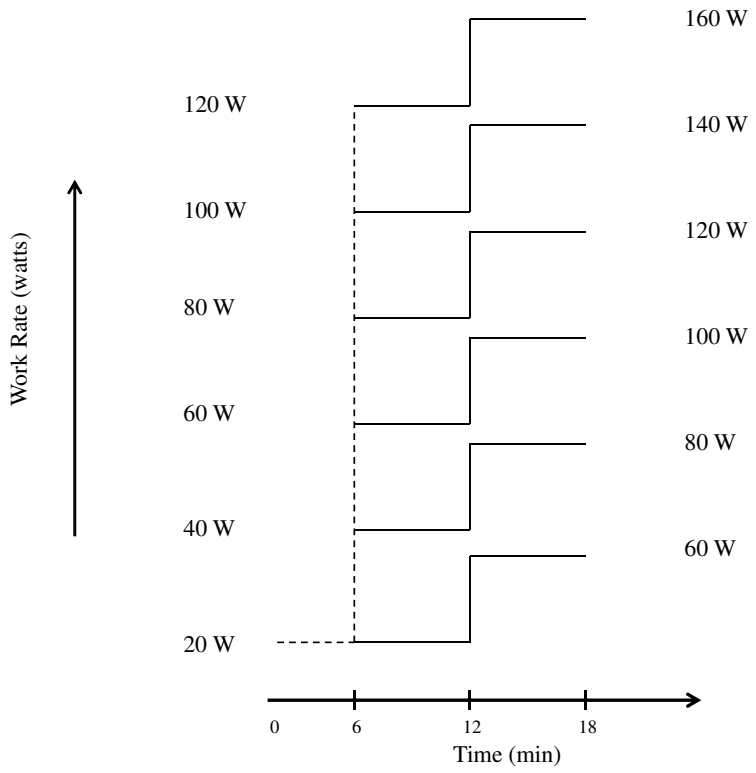
Work Rate (watts)
120 W
100 W
80 W
60 W
40 W
20 W
160 W
140 W
120 W
100 W
80 W
60 W
0
6
12
18
Time (min)

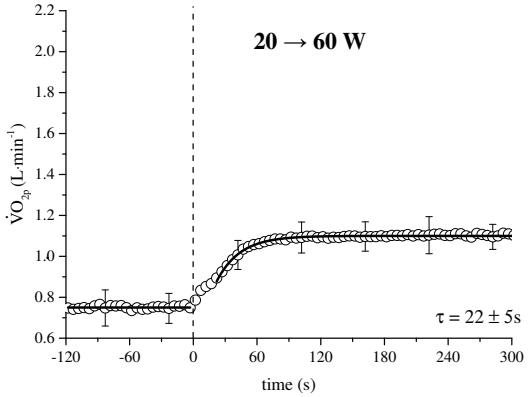
20 → 60 W
τ = 22 ± 5s
$\dot{V}O_{2p}$ (L·min^{-1})
time (s)

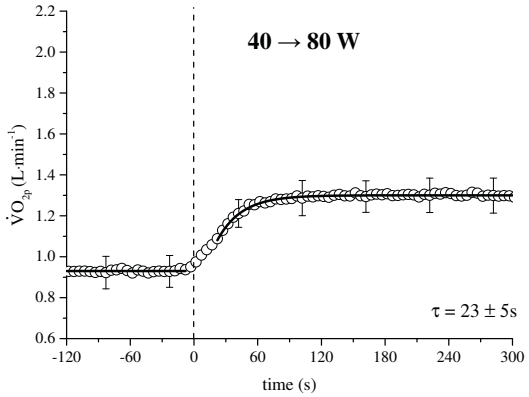
40 → 80 W
τ = 23 ± 5s
$\dot{V}O_{2p}$ (L·min^{-1})
time (s)

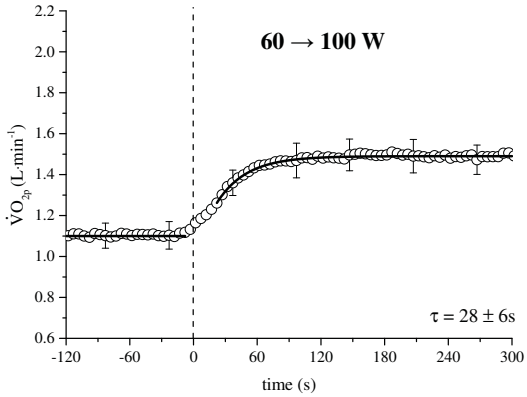
60 → 100 W
τ = 28 ± 6s
$\dot{V}O_{2p}$ (L·min^{-1})
time (s)

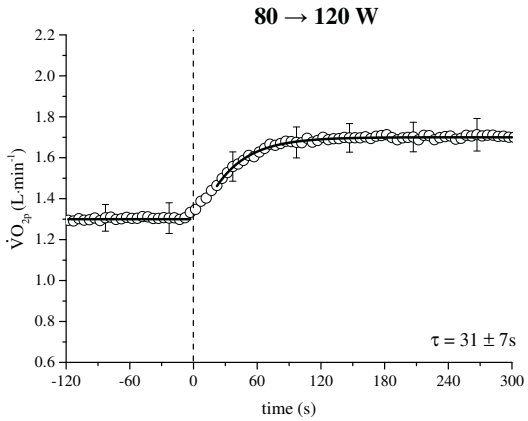
80 → 120 W
τ = 31 ± 7s
$\dot{V}O_{2p}$ (L·min^{-1})
time (s)

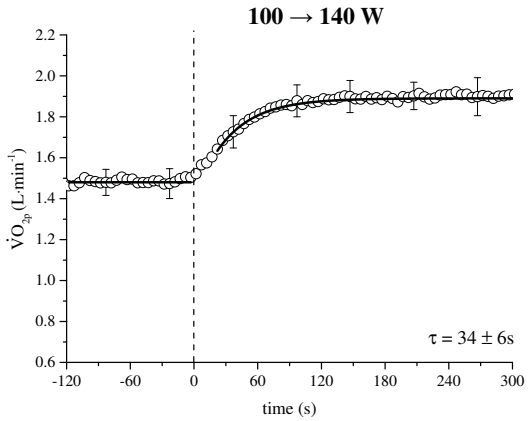
100 → 140 W
τ = 34 ± 6s
$\dot{V}O_{2p}$ (L·min^{-1})
time (s)

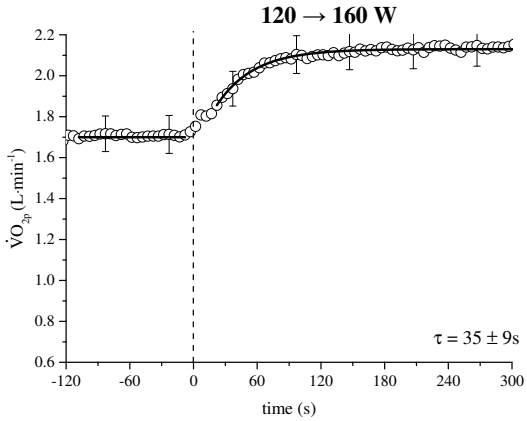
120 → 160 W
τ = 35 ± 9s
$\dot{V}O_{2p}$ (L·min^{-1})
time (s)

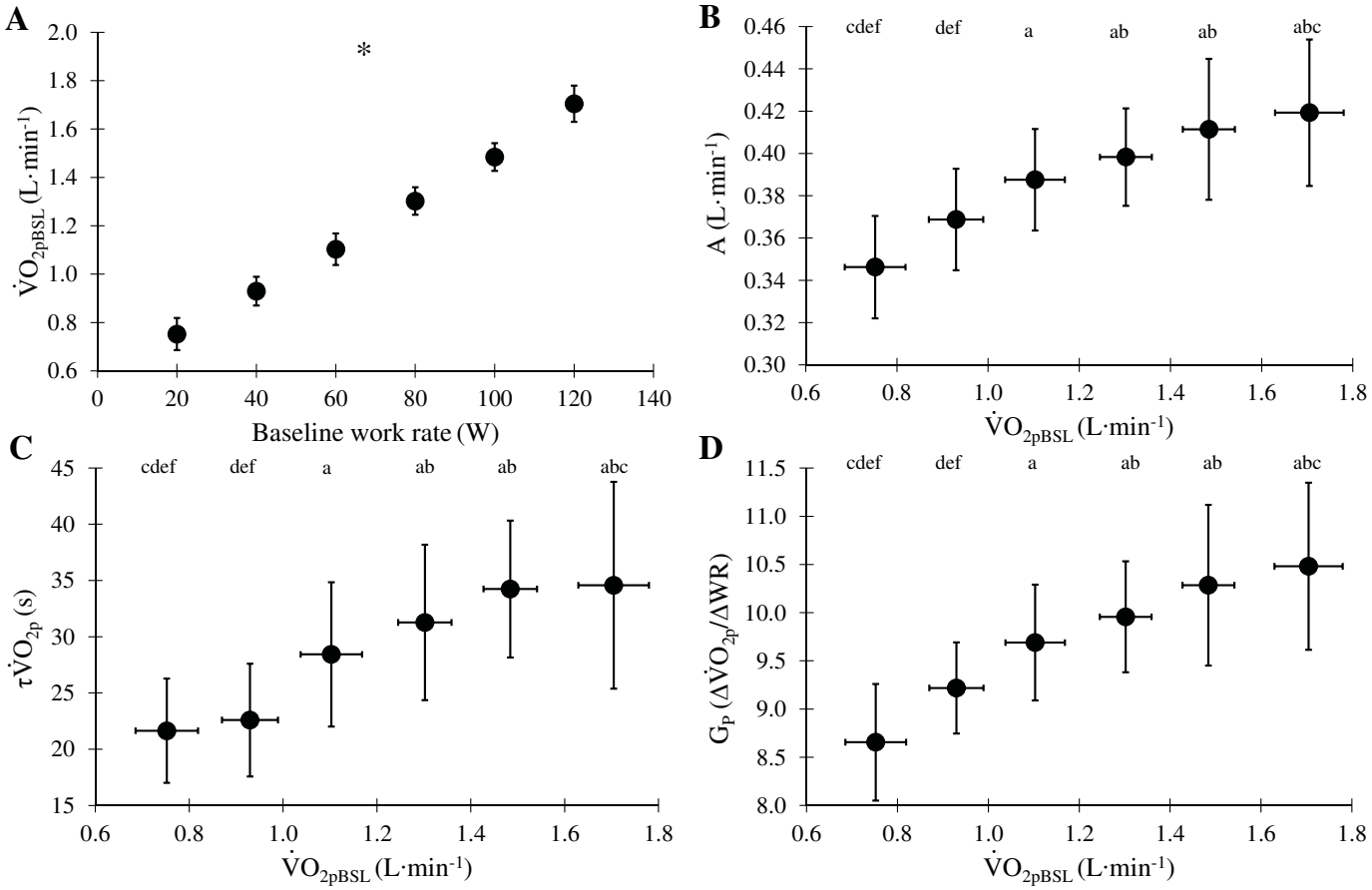
A
B
C
D
*
cdef
def
a
ab
ab
abc
Baseline work rate (W)
$\dot{V}O_{2pBSL}$ (L·min^{-1})
A (L·min^{-1})
$\tau\dot{V}O_{2p}$ (s)
G_p ($\Delta\dot{V}O_{2p}/\Delta WR$)

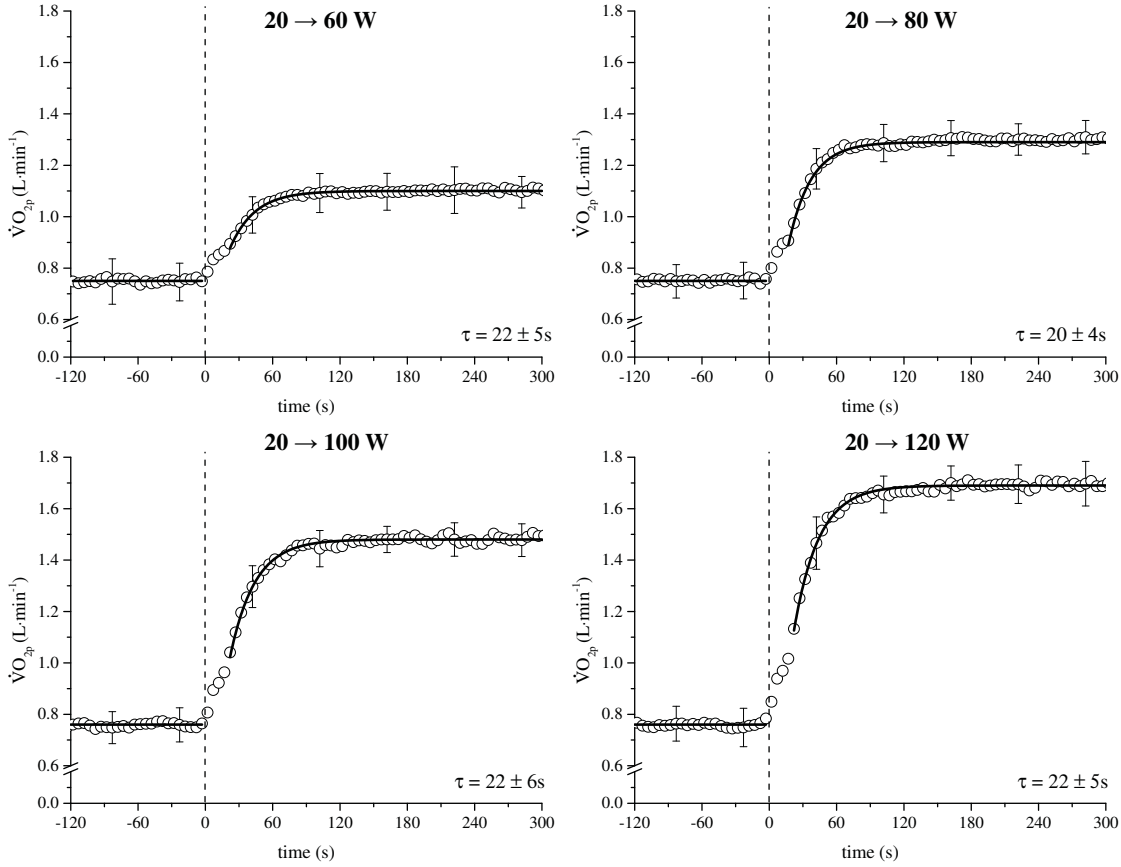
20 → 60 W
τ = 22 ± 5s
20 → 80 W
τ = 20 ± 4s
20 → 100 W
τ = 22 ± 6s
20 → 120 W
τ = 22 ± 5s
V̇O2p (L·min-1)
time (s)

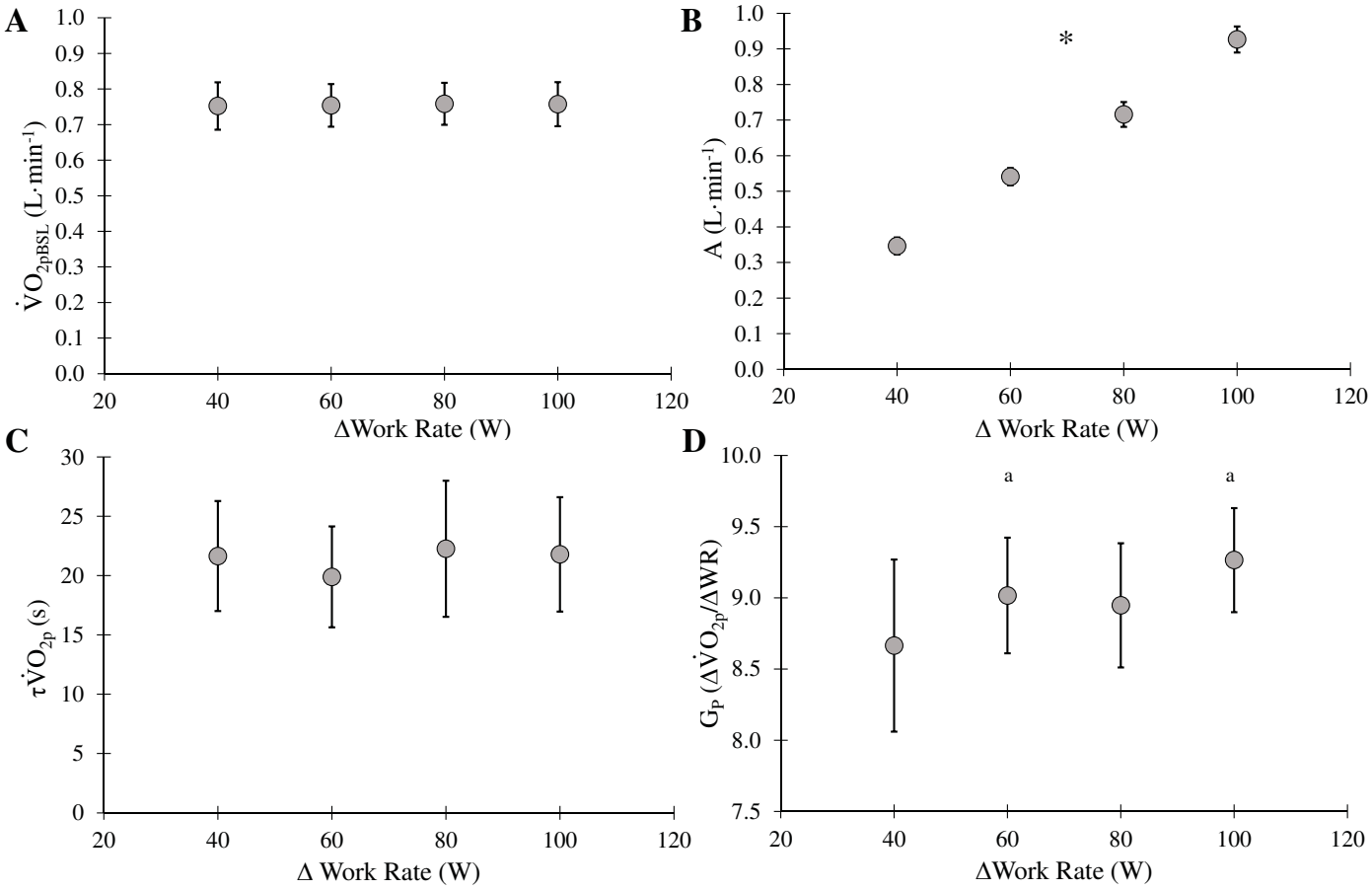
A
$\dot{V}O_{2pBSL}$ (L·min^{-1})
ΔWork Rate (W)
B
A (L·min^{-1})
*
Δ Work Rate (W)
C
$\tau\dot{V}O_{2p}$ (s)
Δ Work Rate (W)
D
G_P ($\Delta\dot{V}O_{2p}/\Delta WR$)
a
a
ΔWork Rate (W)

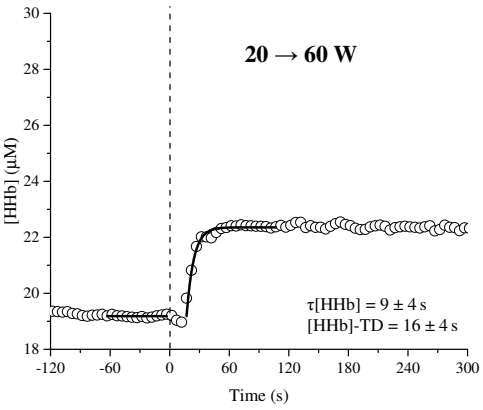
20 → 60 W
[HHb] (µM)
Time (s)
τ[HHb] = 9 ± 4 s
[HHb]-TD = 16 ± 4 s

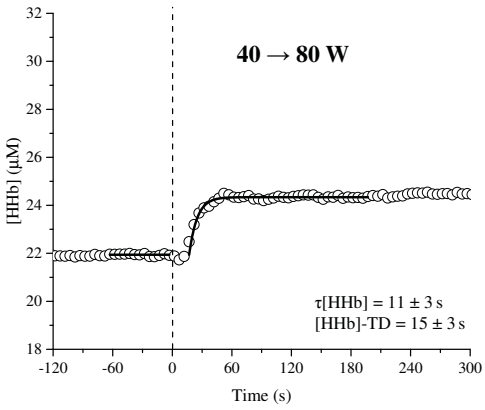
40 → 80 W
[HHb] (µM)
Time (s)
τ[HHb] = 11 ± 3 s
[HHb]-TD = 15 ± 3 s

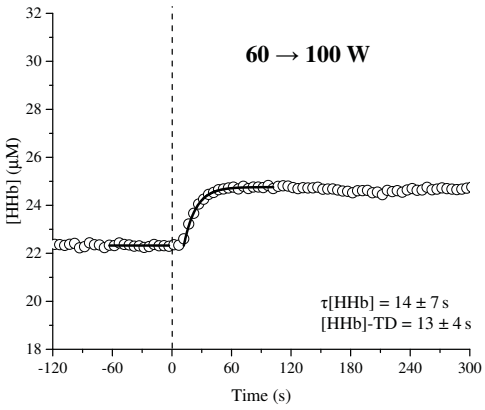
60 → 100 W
[HHb] (µM)
Time (s)
τ[HHb] = 14 ± 7 s
[HHb]-TD = 13 ± 4 s

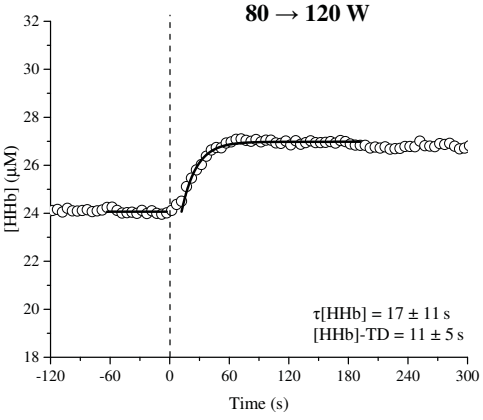
80 → 120 W
[HHb] (µM)
Time (s)
τ[HHb] = 17 ± 11 s
[HHb]-TD = 11 ± 5 s

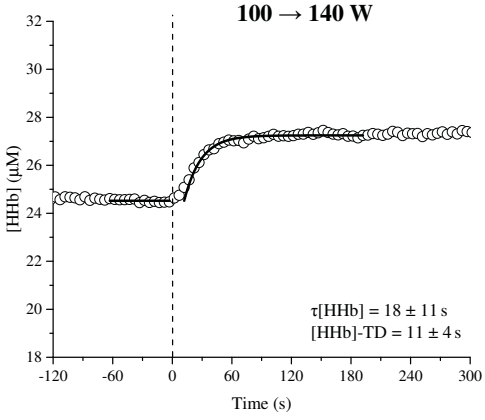
100 → 140 W
[HHb] (µM)
Time (s)
τ[HHb] = 18 ± 11 s
[HHb]-TD = 11 ± 4 s

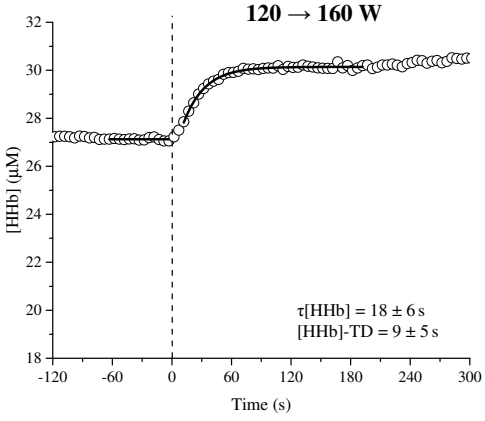
120 → 160 W
[HHb] (µM)
Time (s)
τ[HHb] = 18 ± 6 s
[HHb]-TD = 9 ± 5 s

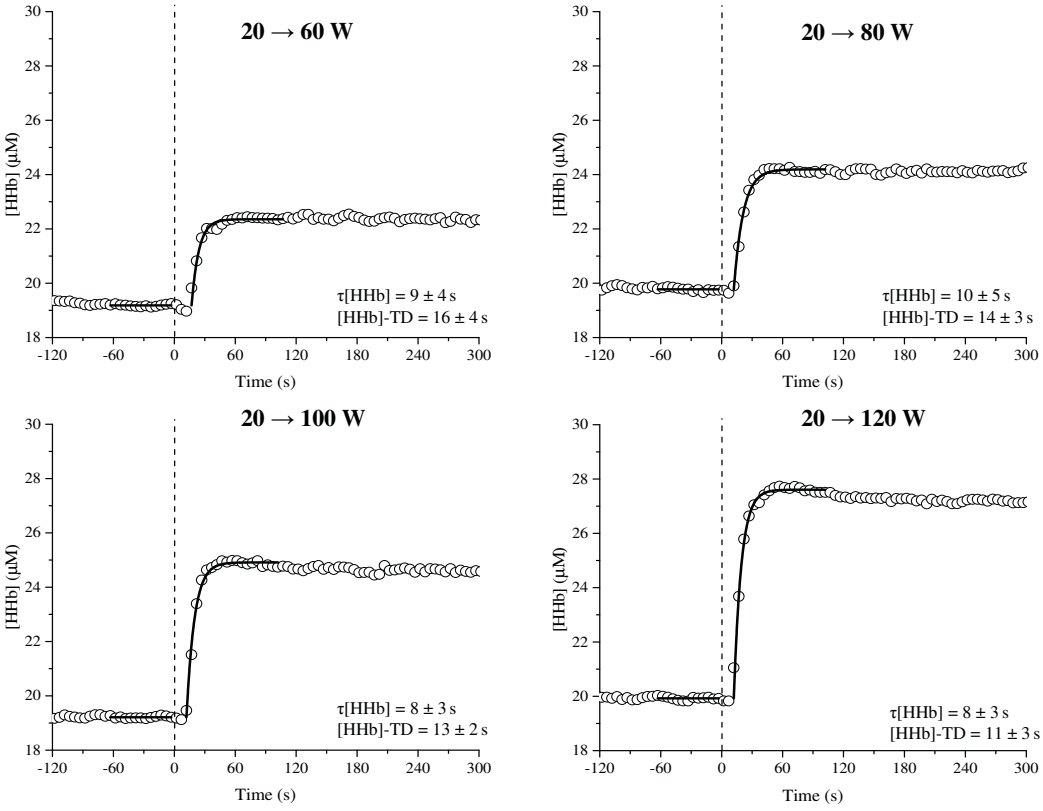
20 → 60 W
[HHb] (μM)
Time (s)
τ[HHb] = 9 ± 4 s
[HHb]-TD = 16 ± 4 s
20 → 80 W
[HHb] (μM)
Time (s)
τ[HHb] = 10 ± 5 s
[HHb]-TD = 14 ± 3 s
20 → 100 W
[HHb] (μM)
Time (s)
τ[HHb] = 8 ± 3 s
[HHb]-TD = 13 ± 2 s
20 → 120 W
[HHb] (μM)
Time (s)
τ[HHb] = 8 ± 3 s
[HHb]-TD = 11 ± 3 s

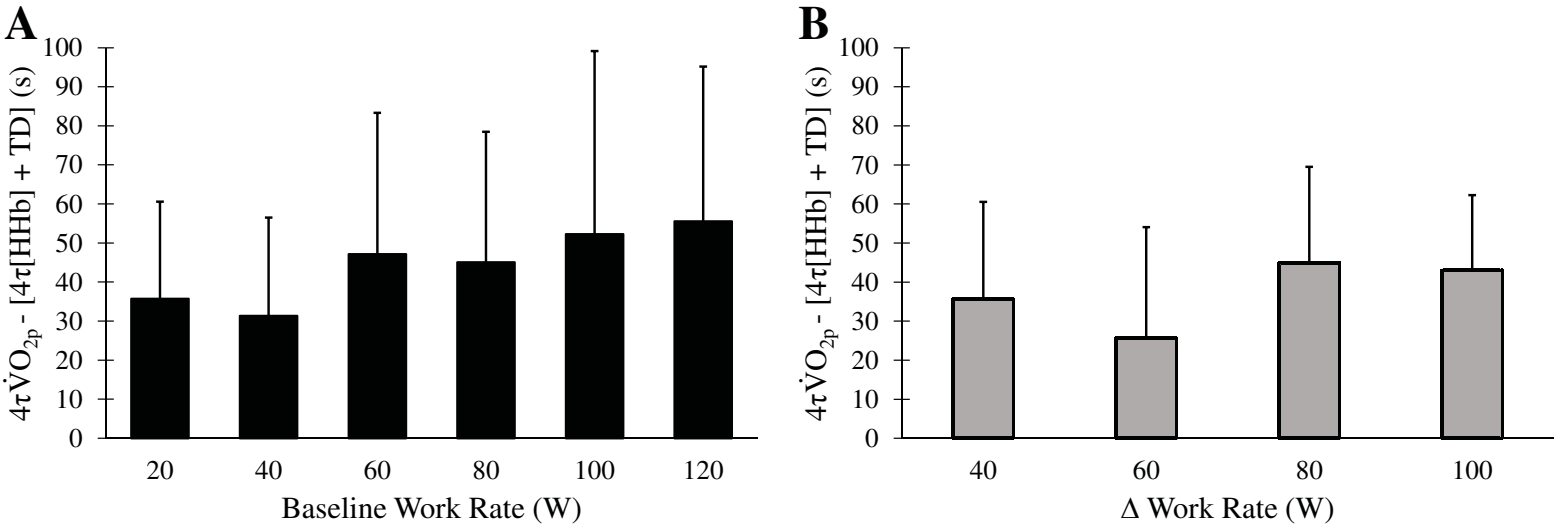
A
B
$4\tau\dot{V}O_{2p}$ - [4τ[HHb] + TD] (s)
0
10
20
30
40
50
60
70
80
90
100
20
40
60
80
100
120
Baseline Work Rate (W)
Δ Work Rate (W)

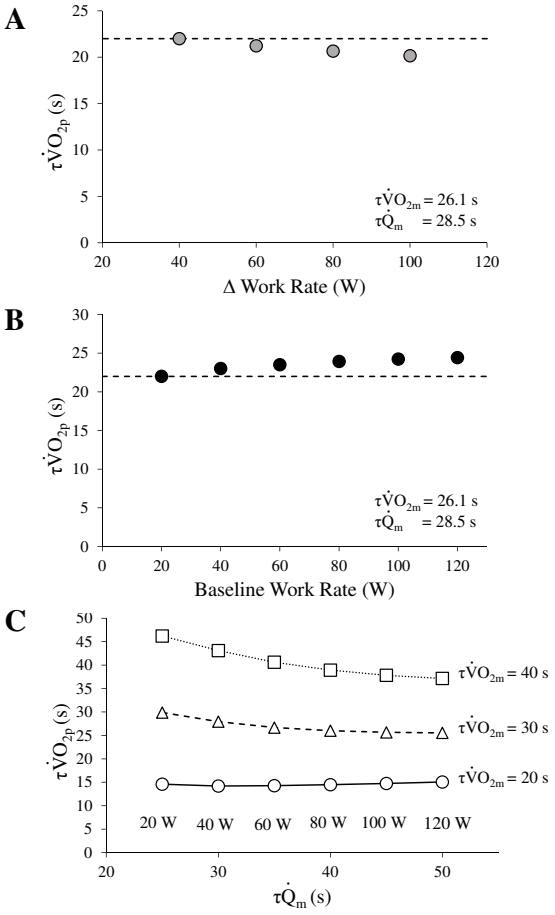
A
τV̇O2p (s)
Δ Work Rate (W)
τV̇O2m = 26.1 s
τQ̇m = 28.5 s
B
τV̇O2p (s)
Baseline Work Rate (W)
τV̇O2m = 26.1 s
τQ̇m = 28.5 s
C
τV̇O2p (s)
τQ̇m (s)
τV̇O2m = 40 s
τV̇O2m = 30 s
τV̇O2m = 20 s
20 W
40 W
60 W
80 W
100 W
120 W

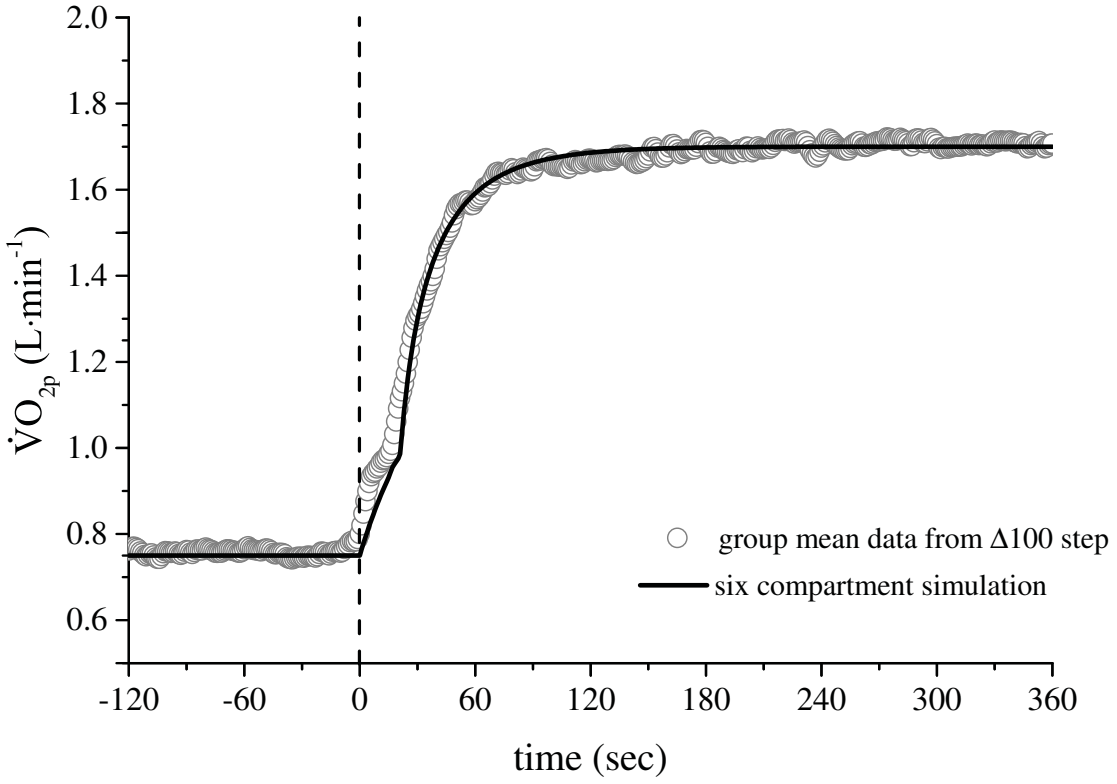
2.0
1.8
1.6
1.4
1.2
1.0
0.8
0.6
$\dot{V}O_{2p}$ (L·min^{-1})
-120
-60
0
60
120
180
240
300
360
time (sec)
group mean data from Δ100 step
six compartment simulation